776

3319

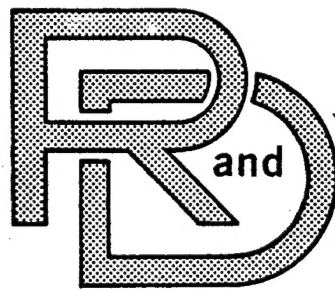# R and D CENTER LABORATORY TECHNICAL REPORT

NO. 12642

A STATE SPACE TECHNIQUE FOR KINEMATIC SYNTHESIS

AND DESIGN OF PLANAR MECHANISMS AND MACHINES

Contract Number DAAK 30-80-C-0042

OCTOBER 1981

Vikram N. Sohoni and Edward J. Haug
College of Engineering
The University of Iowa
Iowa City, IA 52242
University of Iowa Report No. 81-5

by Ronald R. Beck, Project Engineer, TACOM
US Army Tank-Automotive Command
ATTN: DRSTA-ZSA
Warren, MI 48090

2001120 7 068

**U.S. ARMY TANK-AUTOMOTIVE COMMAND
RESEARCH AND DEVELOPMENT CENTER
Warren, Michigan 48090**

NOTICES

The findings in this report are not to be construed as an official Department of the Army position.

Mention of any trade names or manufacturers in this report shall not be construed as advertising nor as an official endorsement of approval of such products or companies by the U.S. Government.

Destroy this report when it is no longer needed. Do not return it to originator.

REPORT DOCUMENTATION PAGE		READ INSTRUCTIONS BEFORE COMPLETING FORM
1. REPORT NUMBER	**2. GOVT ACCESSION NO.**	**3. RECIPIENT'S CATALOG NUMBER**
4. TITLE *(and Subtitle)* A State Space Technique for Kinematic Synthesis and Design of Planar Mechanisms and Machines		**5. TYPE OF REPORT & PERIOD COVERED**
		6. PERFORMING ORG. REPORT NUMBER
7. AUTHOR(s) Vikarm N. Sohoni & Edward J. Haug University of Iowa Ronald R. Beck, TACOM		**8. CONTRACT OR GRANT NUMBER(s)** DAAK-30-80-C-0042
9. PERFORMING ORGANIZATION NAME AND ADDRESS The University of Iowa College of Engineering Iowa City, IA 52242		**10. PROGRAM ELEMENT, PROJECT, TASK AREA & WORK UNIT NUMBERS**
11. CONTROLLING OFFICE NAME AND ADDRESS US Army Tank-Automotive Command R&D Center Tank-Automotive Concepts Lab, DRSTA-ZSA Warren, MI 48090		**12. REPORT DATE** October 1981
		13. NUMBER OF PAGES 129
14. MONITORING AGENCY NAME & ADDRESS*(if different from Controlling Office)*		**15. SECURITY CLASS.** *(of this report)* UNCLASSIFIED
		15a. DECLASSIFICATION/DOWNGRADING SCHEDULE

16. DISTRIBUTION STATEMENT *(of this Report)*

Approved for public release; distribution unlimited.

17. DISTRIBUTION STATEMENT *(of the abstract entered in Block 20, if different from Report)*

18. SUPPLEMENTARY NOTES

19. KEY WORDS *(Continue on reverse side if necessary and identify by block number)*

State Space Technique, Kinematic Synthesis and Design, Mechanism

20. ABSTRACT *(Continue on reverse side if necessary and identify by block number)*

Synthesis of mechanisms to perform kinematic functions has been the subject of a number of investigations. Mechanisms being synthesized in these scheme's are characterized by the requirement that a member generate a path or a function of the input. Optimization of mechanisms for kinetic performance, such as stress-constrained design or force balancing, has been the subject of only a limited number of investigations. Most methods available for synthesis and design of these classes of mechanisms are restricted in applicability to a

very specific class of problems. In the state space technique presented in this report, problems of optimal design of mechanisms are formulated in a setting that allows treatment of general design objectives and constraints. A constrained multielement technique is employed for position, velocity, acceleration, and kineto-static force analysis of mechanisms. An adjoint variable technique is employed to compute derivatives with respect to design of general cost and constraint functions that involve kinematic, force, and design variables. A generalized steepest descent algorithm with constraint compensation is employed, using the design sensitivity analysis method developed, for general-purpose kinematic system optimization. Five optimal design problems are solved to demonstrate effectiveness of the method.

TABLE OF CONTENTS

LIST OF TABLES

LIST OF FIGURES

CHAPTER 1

INTRODUCTION

1.1 Motivation

Design of mechanisms and machines is of major importance in mechanical design. Design techniques currently in use are generally oriented toward design of specific small-scale mechanisms. Some assumptions made in these techniques are often unrealistic. The increasing complexity of mechanisms, as required by machines with automatic and programmable action, requires general-purpose techniques for design of large-scale, multidegree-of-freedom mechanisms.

The purpose of this research is to develop a general-purpose theory for design optimization of mechanisms and machines. An experimental computer code to implement the theory is developed and a number of example problems are considered to demonstrate the wide range of applicability of the technique.

1.2 Existing Methods of Mechanism Synthesis

Synthesis techniques for mechanisms have generally been aimed at designing systems, some member of which is required to either describe a desired path or generate a function of the input. The objective in these design situations is to determine the member lengths and other mechanism parameters to minimize the difference between the desired and actual path or function generated by the mechanism. The precision point

approach and its variants [1,2] have been applied, with success, for solution of these design problems. The basic idea underlying these approaches is to design the mechanism to ensure conformity, within certain tolerances, between the actual path and the desired path, at specified points on the path. The Chebyshev and least square error criteria have been used to characterize the error.

Balancing of mechanisms and machines is another area that has received considerable attention [3,4,5]. The mechanisms being considered in these investigations are generally high-speed inertia variant rotating machinery. Due to the inertia variant nature of the mechanism, the support frame experiences large shaking forces and moments. The design objective is to redistribute mass of links or to add counterweights to minimize shaking forces or moments.

Synthesis of multidegree-of-freedom mechanisms has been the subject of several papers [6,7]. The synthesis technique described in these references was essentially restricted to two-degree-of-freedom mechanisms. Synthesis of a mechanism so that it will occupy less than a prescribed amount of space has been studied in Ref. 8.

In the synthesis methods considered above, constraints have generally been imposed on design variables, such as link lengths, or on generalized coordinates, such as angles between links. Constraints on transmission angle have been extensively used. Methods for stress and deformation constrained design of mechanisms have recently appeared in the literature [9]. Minimum weight design is the objective of these design schemes.

As is evident from the brief survey given in the preceding paragraphs, most available synthesis schemes are oriented toward design of a specific type of mechanism, to perform a specific class of tasks. Some efforts have been made in developing synthesis schemes that are more general than those described above [10,11,12]. The generality of these schemes, however, is limited to a particular class of problems.

1.3 Modeling Techniques for Large-Scale Mechanisms and Machines

Modeling techniques for large-scale dynamic mechanical systems have been developed only in the 1970's [13]. Modeling techniques for dynamic electronic and structural systems, on the other hand, have been available for some time. Two of the modeling methods for dynamic mechanical systems are considered appropriate for modeling kinematic mechanical systems. One of them, the loop closure method [14], is embodied in the computer code IMP [15]. This modeling method has been commonly used for modeling kinematic systems [16]. The other method, the 'constrained multielement formulation', is the basis for computer codes ADAMS [17] and DADS [18,19]. This modeling method involves writing equations of motion for each individual member and then adjoining equations of constraint through Lagrange multipliers. This modeling method, though not yet used for synthesis of kinematic systems, has attractive features for doing so.

1.4 Techniques Available for Design Optimization of Large-Scale Systems

Techniques for design optimization play an important role in kinematic design. Most methods previously employed for optimization of

structural and mechanical systems belong to the field of nonlinear programming, in which the design problem is formulated in terms of design variables that are to be selected. Optimization methods such as the Sequential Unconstrained Minimization Technique (SUMT) [8] and Optimality criteria [9] have been used for Kinematic synthesis. Performance constraints, however, are most naturally stated in terms of state or response variables. Ad hoc techniques have been used to reduce the design problem to a standard nonlinear programming problem, with attendant limitations on generality, analytical feasibility, and computational efficiency.

Numerical methods used in optimal control and optimal design theory [Ref. 20, Ch. 3] sharply contrast those employed in early mechanical system optimization. A state space formulation is employed that explicitly treats design and state variables. The state variable is generally the solution of a matrix or differential equation, for which an adjoint or costate variable is defined as the solution of a related problem. The adjoint variable and the associated adjoint equation are used to provide explicit design sensitivity information. This sensitivity information is required for virtually all iterative methods of design optimization. The state space optimization technique has been successfully applied to design of structural systems. When applied to optimization of large-scale structural systems, this method compares favorably to indirect methods such as optimality criteria [20].

Most mechanical design problems require the system to perform over the range of input or control parameters. In the case of kinematic synthesis of a four-bar path generator mechanism, for example, one could

consider the angular input given to the input link to be the input parameter. At every point in the specified range of the input parameter, design constraints must be satisfied. Most kinematic synthesis problems fall into this class, called worst case or parametric optimal design. This optimal design scheme has been applied with success to design of structural systems and vehicle suspension systems. [Ref. 20, Ch. 5].

1.5 Scope of The Report

In light of the comments made in Sections 1.1 to 1.4, the general conclusion can be drawn that no general-purpose techniques have been developed for mechanism synthesis and design. The level of generality implied in the term 'general purpose' is the ability of techniques to handle large-scale mechanisms, with a variety of constraints and cost functions imposed on the design.

In this report, a technique based on the constrained multielement formulation is developed for modeling planar kinematic systems. The technique is general and is capable of modeling multidegree-of-freedom systems. Velocities and accelerations of the members and reaction forces in joints can also be computed and constrained. A kinetostatic force analysis, as opposed to a time response analysis, is resorted to for computation of the reaction forces. Since the basic assumption of the kinetostatic analysis is that the kinematics of the system are independent of externally applied forces, the dynamic effects due to inertia of the members are also included in the kinetostatic force analysis.

The state space optimization technique is used to develop a general method for design sensitivity analysis. The method allows constraints to be imposed on functions of design and state variables. The design sensitivity information so obtained is used in the gradient projection method for iterative optimization.

CHAPTER 2

KINEMATIC ANALYSIS OF MECHANISMS

2.1 Introduction to the Constrained
Multielement Formulation

Before any mechanism synthesis and design schemes are considered, a technique for kinematic analysis of mechanisms needs to be developed. Development of a general synthesis and design procedure requires that the analysis procedure be general in nature. Techniques used to date have been based on writing algebraic equations for independent loops in a mechanism. These equations typically involve relative position variables of the links of the mechanism. These techniques, though adequate for analysis of closed-loop mechanisms, are not well suited for analysis of open-loop mechanisms.

A technique that has been very successful in modeling large-scale open- and closed-loop mechanical systems is the constrained multielement method [17,18]. This technique, though not yet used for kinematic modeling of mechanisms, has attractive features for doing so. A method for kinematic analysis of mechanisms based on this technique is developed in the following sections.

The modeling philosophy of the constrained multielement (CME) formulation is to embed a local coordinate system in each link of the mechanism or machine. The location of this coordinate system is arbitrary, but is often located at the center of mass. Since only planar systems are being considered in this report, the position and orientation

of any body or link in the system can be described by the three gener-
alized coordinates x_i, y_i and θ_i. These quantities can be represented
by the subvector $q^{(i)}$, where

$$q^{(i)} = \begin{bmatrix} x_i \\ y_i \\ \theta_i \end{bmatrix} \qquad (2.1)$$

As shown in Fig. 2.1, any point p on body i of the system can be
represented by coordinates ξ_{ij} and η_{ij}, conveniently measured in the
local coordinate system. Knowing the generalized coordinates for the
body, it is then possible to express the position of a typical point p
in the global coordinate system.

A mechanical system generally consists of many members, connected
by joints. These joints could be looked upon as constraints imposed on
the relative motion of connected pairs of bodies. The CME formulation
thus represents joints as constraints between bodies making up the
system. These constraints are expressed as algebraic equations invol-
ving the generalized coordinates of the two connected bodies and addi-
tional geometric variables.

2.2 Position Analysis Of Mechanisms

2.2.1 Formulation of State Equation for Position

2.2.1.1 Kinematic Equations of Constraint

Consider a general system of n bodies connected by ℓ independent
joints. Two types of joints (revolute and translation) are considered
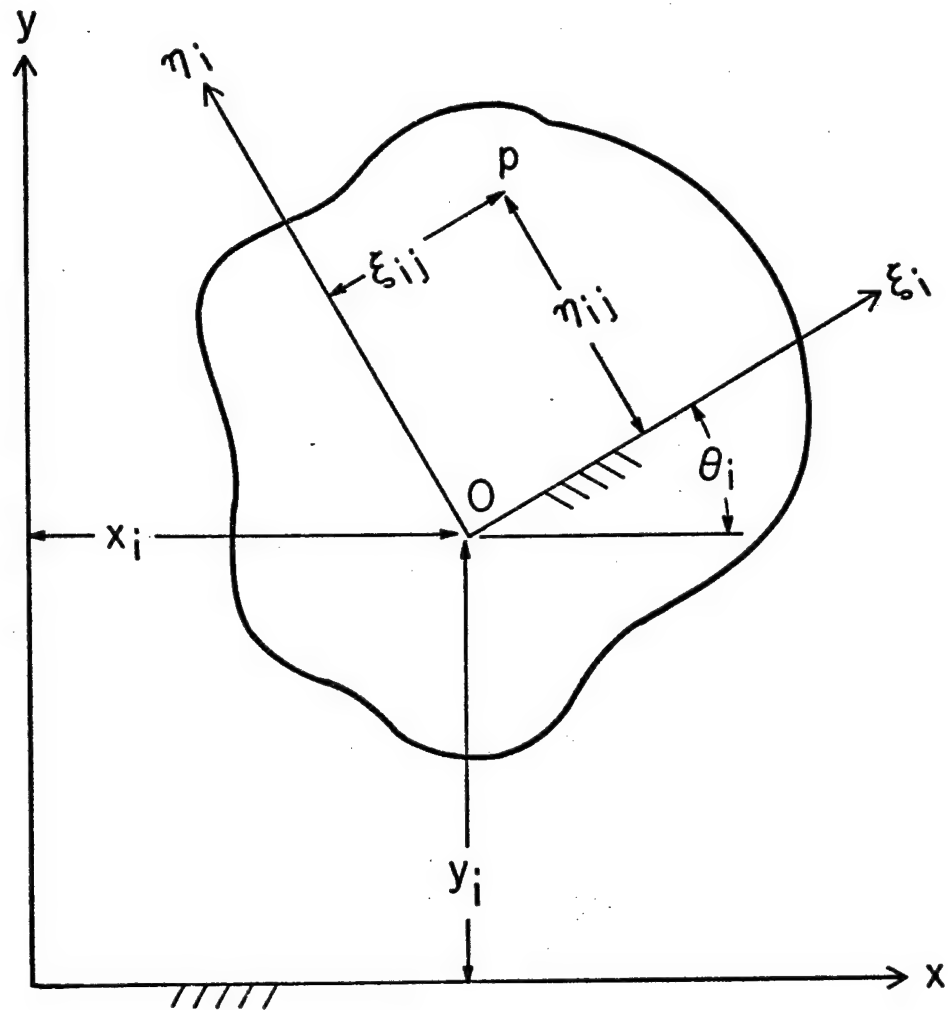
Figure 2.1 Definition of Generalized Coordinates for Body i

in this report, each giving rise to two equations of constraint. These equations of constraint express conditions that the motion of the two connected bodies must satisfy to be compatible with the joint.

A system of n bodies in the plane has a total of 3n generalized coordinates. However, if this system has ℓ independent joints, there are 2ℓ equations of constraint between the 3n generalized coordinates. Thus the number of free-degrees-of-freedom can be written as

$$m = 3n - 2\ell \tag{2.2}$$

where

n = number of bodies in the system

ℓ = number of independent joints in the system

The condition $m > 0$ must be satisfied by all kinematic systems. The generalized coordinates for the entire system can be denoted by the position state vector $z \in R^{3n}$, where

$$z = \begin{Bmatrix} q^{(1)} \\ q^{(2)} \\ \vdots \\ q^{(n)} \end{Bmatrix} \tag{2.3}$$

Assuming that the system has a set of specified design variables $b \in R^s$, the kinematic equations of constraint can be written as

$$\Phi^k(z,b) = 0 \tag{2.4}$$

where

$$\overset{k}{\Phi}(z,b) = \begin{bmatrix} \overset{k}{\phi}_1(z,b) \\ \\ \overset{k}{\phi}_2(z,b) \\ \cdot \\ \cdot \\ \cdot \\ \overset{k}{\phi}_{2\ell}(z,b) \end{bmatrix}$$

$\overset{k}{\phi}_{2i-1}(z,b)$ is the first kinematic constraint due to joint i and $\overset{k}{\phi}_{2i}(z,b)$ is the second kinematic constraint due to joint i.

2.2.1.2 Kinematic Driving Equations

Equation 2.4 as presented in the preceding section, is a system of 2ℓ equations in 3n variables. Since for a kinematic system $3n > 2\ell$, Eq. 2.4 is a system of fewer equations than unknowns. To solve for z from Eq. 2.4, m additional equations are required. These equations can be developed by observing that the basic purpose of designing kinematic systems is to obtain a system that transmits motion from input links to output links. The mechanism or machine can only be given input motion through a set of free degrees of freedom. These free degrees of freedom can thus be specified as functions of some free parameter, or may be specified by some relationship between the 3n state variables. Since all the free degrees of freedom must be specified, to drive the mechanism in a unique way, m additional driving equations of constraints arise, in the form

$$\overset{d}{\Phi}(z,b,\alpha) = 0 \tag{2.5}$$

where

$$\Phi^d(z,b,\alpha) = \begin{bmatrix} \phi^d_1(z,b,\alpha) \\ \cdot \\ \cdot \\ \cdot \\ \phi^d_m(z,b,\alpha) \end{bmatrix}$$

$\alpha \in R^p$ is a vector of input parameters, and $\phi^d_i(z,b,\alpha)$ represents the ith driving equation.

2.2.1.3 State Equation for Position

Combining Eqs. 2.4 and 2.5, one has 3n independent equations, which may be written as

$$\Phi(z,b,\alpha) = \begin{bmatrix} \Phi^k(z,b) \\ \\ \Phi^d(z,b,\alpha) \end{bmatrix} = 0 \tag{2.6}$$

Equation 2.6 is the state equation for position of the mechanism. Specifying the design variable vector b and the input parameter vector α makes Eq. 2.6 a system of 3n independent equations in 3n unknowns, $z \in R^{3n}$. Since these equations are highly nonlinear, more than one solution for z is possible. Conversely, for some designs and inputs, no solution may exist.

2.2.2. Kinematic Constraint Equations

Before any technique is considered for the solution of Eq. 2.6, it is necessary to determine the explicit form of the equations constituting this system of equations. Since kinematic equations of constraint occur in a general form; i.e., the equations of constraint for all

joints of the same type have the same general form, it is sufficient to
consider a typical joint of each type. Since this report considers only
revolute and translation joints, a typical joint of each type will be
treated. Driving constraints, on the other hand, do not lend them-
selves to the same general characterization. These constraints tend
to be problem dependent.

2.2.2.1 Constraint Equations for a Revolute Joint

Figure 2.2 shows the two adjacent bodies i and j, with body-fixed
coordinate systems $O_i x_i y_i$ and $O_j x_j y_j$, respectively. The origins of
these reference frames are located in the global reference frame by
vectors $\overline{R}_i$ and $\overline{R}_j$, respectively. Let point p_{ij} on body i be located by
a body-fixed vector $\overline{r}_{ij}$ and point p_{ji} on body j be located by a body
fixed vector $\overline{r}_{ji}$. Points p_{ij} and p_{ji} are, in turn, connected by a
vector $\overline{r}_p$. Executing a closed path from the origin of the fixed
reference frame yields the vector relationship.

$$\overline{R}_i + \overline{r}_{ij} + \overline{r}_p - \overline{r}_{ji} - \overline{R}_j = \overline{0} \tag{2.7}$$

Demanding that points p_{ij} and p_{ji} are coincident guarantees the
existence of a rotational joint between bodies i and j at this common
point. This is equivalent to the condition $\overline{r}_p = \overline{0}$. Thus, Eq. 2.7
becomes

$$\overline{R}_i + \overline{r}_{ij} - \overline{r}_{ji} - \overline{R}_j = \overline{0} \tag{2.8}$$

In matrix form, Eq. 2.8 can be written as
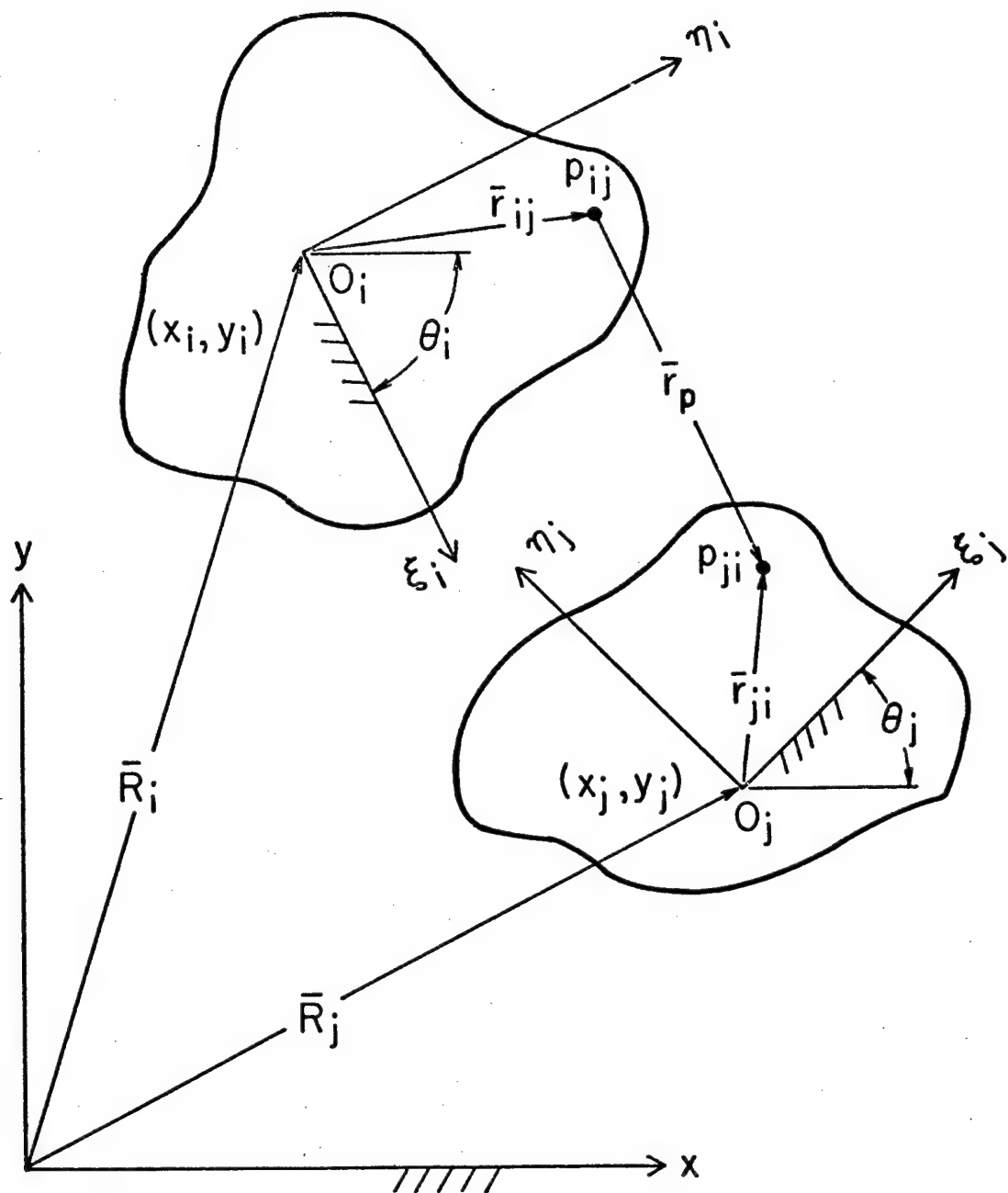
Figure 2.2   Revolute Joint

$$
\begin{bmatrix} x_i \\ y_i \end{bmatrix} + E(\theta_i) \begin{bmatrix} \xi_{ij} \\ \eta_{ij} \end{bmatrix} - \begin{bmatrix} x_j \\ y_j \end{bmatrix} - E(\theta_j) \begin{bmatrix} \xi_{ji} \\ \eta_{ji} \end{bmatrix} = \begin{bmatrix} 0 \\ 0 \end{bmatrix} \qquad (2.9)
$$

where

$$
E(\theta) = \begin{bmatrix} \cos\theta & -\sin\theta \\ \sin\theta & \cos\theta \end{bmatrix}
$$

is a rotation matrix from the local to global reference frame.

Expanding Eq. 2.9, the equations of constraint for the revolute joint can be written as

$$
\phi_x = x_i + \xi_{ij}\cos\theta_i - \eta_{ij}\sin\theta_i - x_j - \xi_{ji}\cos\theta_j + \eta_{ji}\sin\theta_j = 0
$$

$$
\phi_y = y_i + \xi_{ij}\sin\theta_i + \eta_{ij}\cos\theta_i - y_j - \xi_{ji}\sin\theta_j - \eta_{ji}\cos\theta_j = 0
$$

$$
(2.10)
$$

In Eq. 2.10, x_i, y_i, θ_i, x_j, y_j, and θ_j are state variables. The variables ξ_{ij}, η_{ij}, ξ_{ji}, and η_{ji} are related to the length of the members and hence to the design variables.

2.2.2.2 Constraint Equations for a Translational Joint

Figure 2.3 shows two bodies connected by a translational joint. For this type of joint, the points p_{ij} and p_{ji} lie on a line parallel to the path of relative motion between the two bodies. These points are located by nonzero body-fixed vectors, $\bar{r}_{ij}$ and $\bar{r}_{ji}$, that are perpendicular to the line of relative motion. A scalar equation of constraint can be written by taking the dot product of $\bar{r}_{ij}$ with $\bar{r}_p$. Since these two vectors are perpendicular, their dot product must vanish.
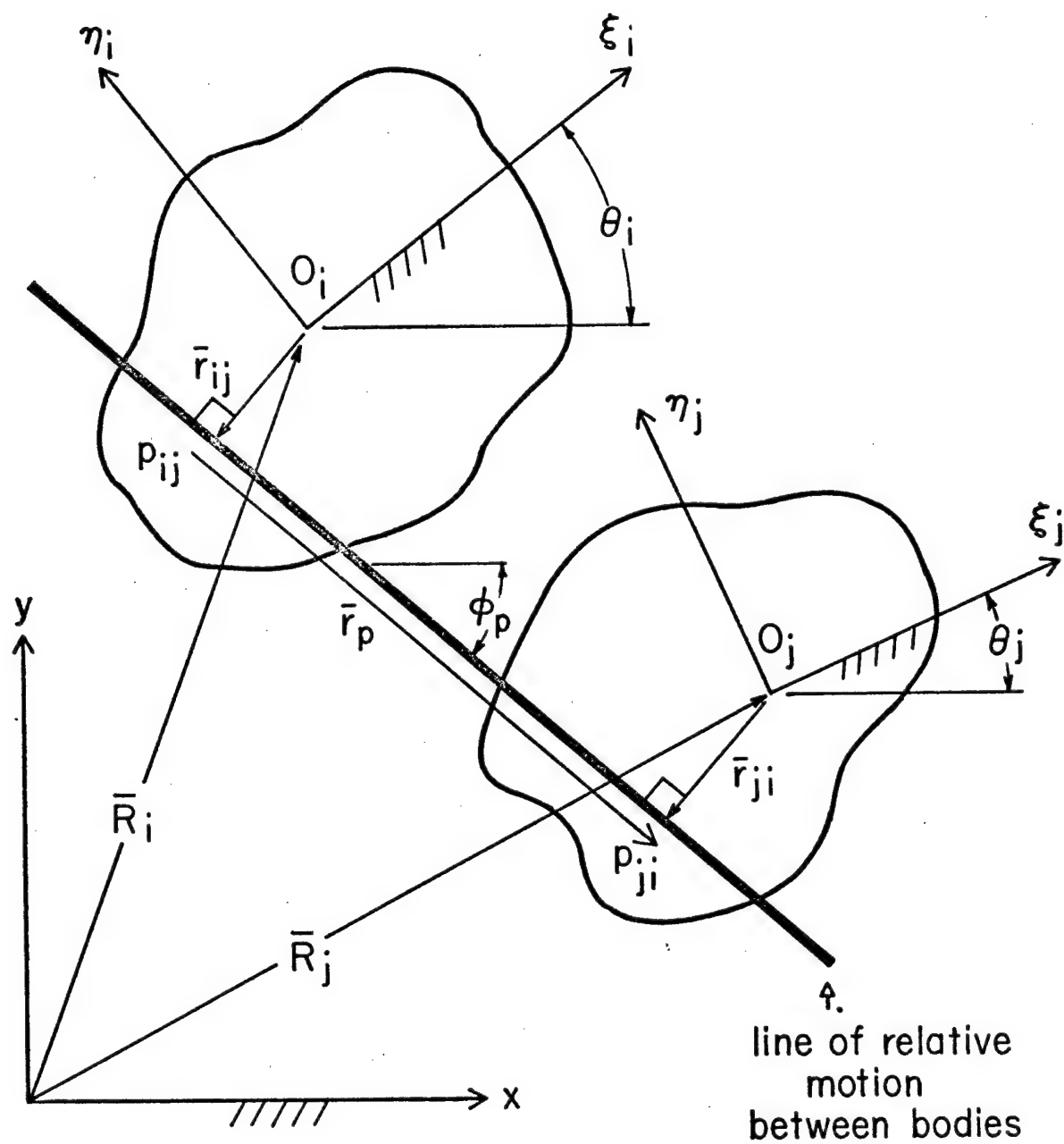
Figure 2.3   Translation Joint

$$\overline{r}_p \cdot \overline{r}_{ij} = 0 \tag{2.11}$$

Using Eq. 2.7 to solve for $\overline{r}_p$, Eq. 2.11 becomes

$$(\overline{R}_j + \overline{r}_{ji}) - (\overline{R}_i + \overline{r}_{ij}) \cdot \overline{r}_{ij} = 0 \tag{2.12}$$

Using the transformation matrix to express $\overline{r}_{ji}$ and $\overline{r}_{ij}$ in the global reference frame, Eq. 2.12 can be written as

$$\phi_n = (U_i - x_i)(U_i - U_j) + (V_i - y_i)(V_i - V_j) = 0 \tag{2.13}$$

where

$$U_i = x_i + \xi_{ij} \cos \theta_i - \eta_{ij} \sin \theta_i$$

$$U_j = x_j + \xi_{ji} \cos \theta_j - \eta_{ji} \sin \theta_j$$

$$\tag{2.14}$$

$$V_i = y_i + \xi_{ij} \sin \theta_i + \eta_{ij} \cos \theta_i$$

$$V_j = y_j + \xi_{ji} \sin \theta_j + \eta_{ji} \cos \theta_j$$

Equation 2.13 restricts the motion of body i to be along a line that is at a specified distance from and parallel to the line of relative motion.

The second scalar equation of constraint can be obtained by noting that $\overline{r}_{ij}$ and $\overline{r}_{ji}$ must be parallel. This is true since both of these vectors are perpendicular to $\overline{r}_p$. In three dimensions, this condition can be expressed as

$$\overline{r}_{ij} \times \overline{r}_{ji} = \overline{0} \tag{2.15}$$

Expanding, the component perpendicular to the x-y plane is

$$\phi_\theta = (U_i - x_i)(V_j - y_j) - (V_i - y_i)(U_j - x_j) = 0 \tag{2.16}$$

Since body i is constrained by Eq. 2.13 to move parallel to $\bar{r}_p$, Eq. 2.16 guarantees that body j will also move along a line parallel to $\bar{r}_p$. As in the case of the revolute joint, x_i, y_i, θ_i, x_j, y_j, and θ_j are the state variables in the equations of constraint. Variables ξ_{ij}, η_{ij}, ξ_{ji}, and η_{ji} and related to the design variables.

2.2.3 Solution Technique for State Equations

Constraint equations for the two typical joints considered here, Eqs. 2.10, 2.13, and 2.16, are geometrically nonlinear, due to the presence of transcendental functions of state variables. The position state equation is thus nonlinear and a solution technique that is applicable to nonlinear equations must be employed. One of the commonly used techniques for solution of nonlinear equations is Newton's method [21].

Consider the position state equation of Eq. 2.6 for the entire system,

$$\Phi(z,b,\alpha) = 0$$

Before any attempt is made to solve this nonlinear system, variables b and α must be specified. This is reasonable, since in most iterative design algorithms the design variable b is estimated before the synthesis procedure is initiated. The vector of input parameters α is generally a part of the problem specifications. The only unknowns in Eq. 2.6 are the state variables z. Equation 2.6 is thus a system of 3n nonlinear equations in 3n variables and a unique solution of this system will exist locally if the stipulations of the implicit function theorem are satisfied; ie., if the matrix

$$\frac{\partial \Phi(z,b,\alpha)}{\partial z} = \begin{bmatrix} \dfrac{\partial \phi_i}{\partial z} \\[2mm] j \end{bmatrix}_{3n \times 3n} \qquad (2.17)$$

is nonsingular. This condition is satisfied if the system of constraints consists of no redundant joints.

The Newton method [21] initially requires that the state variable z be estimated. The method then computes updates Δz to this state to obtain an improved value for the state. The improved approximation is given by [21]

$$z^{(i+1)} = z^{(i)} + \Delta z^{(i)} \qquad (2.18)$$

where i is an iteration counter, $i > 0$,

$\Delta z^{(i)}$ is the solution of

$$\frac{\partial \Phi}{\partial z} (z^i,b,\alpha)\ \Delta z^i = - \Phi(z^i,b,\alpha) \qquad (2.19)$$

and the matrix $[\partial \Phi/\partial z]$ is called the Jacobian matrix of the system.

For large mechanisms, the system of Eq. 2.6 can be quite large, giving rise to a large system of linear equations in Eq. 2.19. Examining the kinematic constraint equations for the two types of joints, Eqs. 2.10, 2.13 and 2.16, it can be concluded that these pairs of constraint equations involve only the state variables of the two bodies that they connect. These equations are thus weakly coupled and the Jacobian matrix in the left-hand side of Eq. 2.19 is highly sparse. Efficient sparse matrix codes [22] can thus be used for solution of Eq. 2.19.

Repeated solution of systems of equations similar to Eq. 2.19 are required very often in the following chapters. To perform these

computations efficiently, the sparse matrix code initially does a symbolic LU factorization of the coefficient matrix. Subsequent solutions of linear systems with the same coefficient matrix, but with different right-hand sides, can be carried out very efficiently.

Since mechanisms are being synthesized to perform over a range of input parameters α, solution of the state equations would be required at specific values of α. The process of obtaining the solution of the position state equation for a specified value of α can be repeated to obtain the solution for a desired sequence of input variables α^j. The numerical efficiency of such a sequence of calculations is very good if α^{j+1} is close to α^j, since $z(\alpha^j)$ serves as a good starting estimate in the computation of $z(\alpha^{j+1})$. If, however, α^{j+1} and α^j are not close, then an update $\delta z(\alpha^j)$ to $z(\alpha^j)$ is required to produce a reasonable estimate for this computation. One such update can be obtained by linearizing the position state equation of Eq. 2.6, keeping b fixed.

$$\frac{\partial \Phi(z,b,\alpha^j)}{\partial z} \ \delta z(\alpha^j) \ + \ \frac{\partial \Phi(z,b,\alpha^j)}{\partial \alpha} \ \delta_\alpha \ = \ 0$$

or

$$\frac{\partial \Phi(z,b,\alpha^j)}{\partial z} \ \delta z(\alpha^j) \ = \ - \ \frac{\partial \Phi(z,b,\alpha^j)}{\partial \alpha} \ \delta_\alpha \tag{2.20}$$

where $\delta\alpha = \alpha^{j+1} - \alpha^j$.

An improved estimate for $z(\alpha^{j+1})$ can thus be written as

$$z^0(\alpha^{j+1}) = z(\alpha^j) + \ \delta z(\alpha^j) \tag{2.21}$$

where $\delta z(\alpha^j)$ is the solution of Eq. 2.20. Equation 2.20 has the same coefficient matrix as Eq. 2.19, so its numerical solution is quite efficient.

2.3 Velocity Analysis Of Mechanisms

Most mechanisms are driven by input sources that give input links of the mechanism finite velocity. It is then necessary to determine velocities of the remaining links in the mechanism, during motion of the mechanism, over the prescribed range of inputs.

The state equation for the mechanism, Eq. 2.6, is required to hold for all time. It can, therefore, be differentiated with respect to time to obtain

$$\frac{d}{dt} \Phi(z,b,\alpha) = \frac{\partial \Phi(z,b,\alpha)}{\partial z} \dot{z} + \frac{\partial \Phi(z,b,\alpha)}{\partial \alpha} \dot{\alpha} = 0 \qquad (2.22)$$

The above equation can be rewritten as

$$\left[\frac{\partial \Phi(z,b,\alpha)}{\partial z} \right] \dot{z} = - \frac{\partial \Phi(z,b,\alpha)}{\partial \alpha} \dot{\alpha} \qquad (2.23)$$

where $\dot{z} \in R^{3n}$ is the vector of generalized velocities of members of the system.

Equation 2.23 is the velocity state equation. This equation is linear in velocities and has the same coefficient matrix as Eq. 2.19. As stated in section 2.2.3, this matrix is sparse and its symbolically factorized LU form has been determined and stored. The solution of Eq. 2.23 is thus the same as solving Eq. 2.19, with a different right-hand side. The solution of this equation is thus very efficient.

The components of the vector on the right side of Eq. 2.23 are not so obvious. Time does not explicitly appear in the kinematic constraint equations. However, in the driving equations, the input parameter α could be given as an explicit function of time. The partial derivative

of Eq. 2.6 with respect to time can be written as

$$\frac{\partial \Phi(z,b,\alpha)}{\partial \alpha} \dot{\alpha} = \begin{bmatrix} \dfrac{\partial \Phi^k(z,b)}{\partial \alpha} \dot{\alpha} \\[3mm] \dfrac{\partial \Phi^d(z,b,\alpha)}{\partial \alpha} \dot{\alpha} \end{bmatrix} \tag{2.24}$$

Since the kinematic constraints $\Phi^k = 0$ do not depend explicitly on α, Eq. 2.24 can be rewritten as

$$\frac{\partial \Phi(z,b,\alpha)}{\partial \alpha} \dot{\alpha} = \begin{bmatrix} \overline{0} \\[3mm] \dfrac{\partial \Phi^d(z,b,\alpha)}{\partial \alpha} \dot{\alpha} \end{bmatrix} \tag{2.25}$$

where $\dot{\alpha} \in R^p$ is the vector of first time derivative of input parameters. The matrix $\dfrac{\partial \Phi^d(z,b,\alpha)}{\partial \alpha}$ in Eq. 2.25 depends on the form of the driving constraints, so it will generally be problem dependent.

2.4 Acceleration Analysis of Mechanisms

Whenever a velocity input is supplied to a mechanism, some links experience accelerations. This is true even if the inputs to the mechanism occur at constant velocity. Computation of accelerations is important, since the forces experienced by links in the mechanism depend directly on acceleration.

As noted in Section 2.3, the position state equations of Eq. 2.6 are required to hold over the entire range of inputs, so the velocity state equation of Eq. 2.23 can be differentiated once again with respect to time to obtain,

$$\frac{d^2}{dt^2} \, \Phi(z,b,\alpha) \;=\; \left[\frac{\partial \Phi(z,b,\alpha)}{\partial z}\right] \ddot{z} + \left[\frac{\partial}{\partial z}\left[\frac{\partial \Phi(z,b,\alpha)}{\partial z}\, \dot{z}\right]\dot{z}\right] + \Omega = 0$$

(2.26)

Equation 2.26 can be written as

$$\left[\frac{\partial \Phi(z,b,\alpha)}{\partial z}\right]\ddot{z} = -\left[\frac{\partial}{\partial z}\left[\frac{\partial \Phi(z,b,\alpha)}{\partial z}\,\dot{z}\right]\dot{z}\right] - \Omega$$

(2.27)

where

$$\Omega = \frac{\partial}{\partial z}\left[\frac{\partial \Phi(z,b,\alpha)}{\partial \alpha}\,\dot{\alpha}\right]\dot{\alpha} + \frac{\partial \Phi(z,b,\alpha)}{\partial \alpha}\,\ddot{\alpha}$$

$\ddot{\alpha} \in R^p$ is the vector of second-time derivatives of input parameters and $\ddot{z} \in R^{3n}$ is the vector of generalized accelerations.

Equation 2.27 is the acceleration state equation. This is a system of linear equations with the same coefficient matrix as Eq. 2.19. All the desirable properties of this coefficient matrix, as stated in section 2.3, still hold. The solution of Eq. 2.27 is thus efficient.

The right-hand side of Eq. 2.27 involves $\dot{z}$, which requires that the velocity state equation of Eq. 2.23 be solved before Eq. 2.27 can be solved. The second term in the right side of Eq. 2.27 involves derivatives of constraints with respect to time. Differentiating Eq. 2.25 with respect to time gives

$$\Omega = \begin{bmatrix} \overline{0} \\[2em] \dfrac{\partial}{\partial \alpha}\left[\dfrac{\partial \Phi^d(z,b,\alpha)}{\partial \alpha}\,\dot{\alpha}\right]\dot{\alpha} \;+\; \left[\dfrac{\partial \Phi^d(z,b,\alpha)}{\partial \alpha}\right]\ddot{\alpha} \end{bmatrix}$$

(2.28)

CHAPTER 3

FORCE ANALYSIS OF MECHANISMS

For realistic design of mechanisms, it is necessary to impose stress constraints on links and force constraints on joint bearings. This requires that a force equation be derived to express internal forces on links, in terms of the externally applied forces and system velocities and accelerations. The applied forces could be forces due to gravity, spring damper actuator forces, or forces from other external sources. Two approaches are taken to arrive at the force equations. It is also shown that these two approaches essentially lead to the same equations for equilibrium.

3.1 Equilibrium Equation from the Principle of Virtual Work

Figure 3.1 shows a body with a body-fixed coordinate system $O_i x_i y_i$. An externally applied force $\overline{F}_{ik}$ and an external moment $\overline{T}_{i\ell}$ act on this body. The point of application of force $\overline{F}_{ik}$ is located by the vector $\overline{S}_{ik}$ in the body-fixed coordinate system. The virtual work of all external forces acting on body i can be written as [23]

$$\delta w_i = \sum_{k=1}^{N_i} \overline{F}_{ik} \cdot \delta(\overline{R}_i + \overline{S}_{ik}) + \sum_{\ell=1}^{M_i} \overline{T}_{i\ell} \cdot \delta\overline{\theta}_i \qquad (3.1)$$

where

N_i = Total number of forces acting on body i.
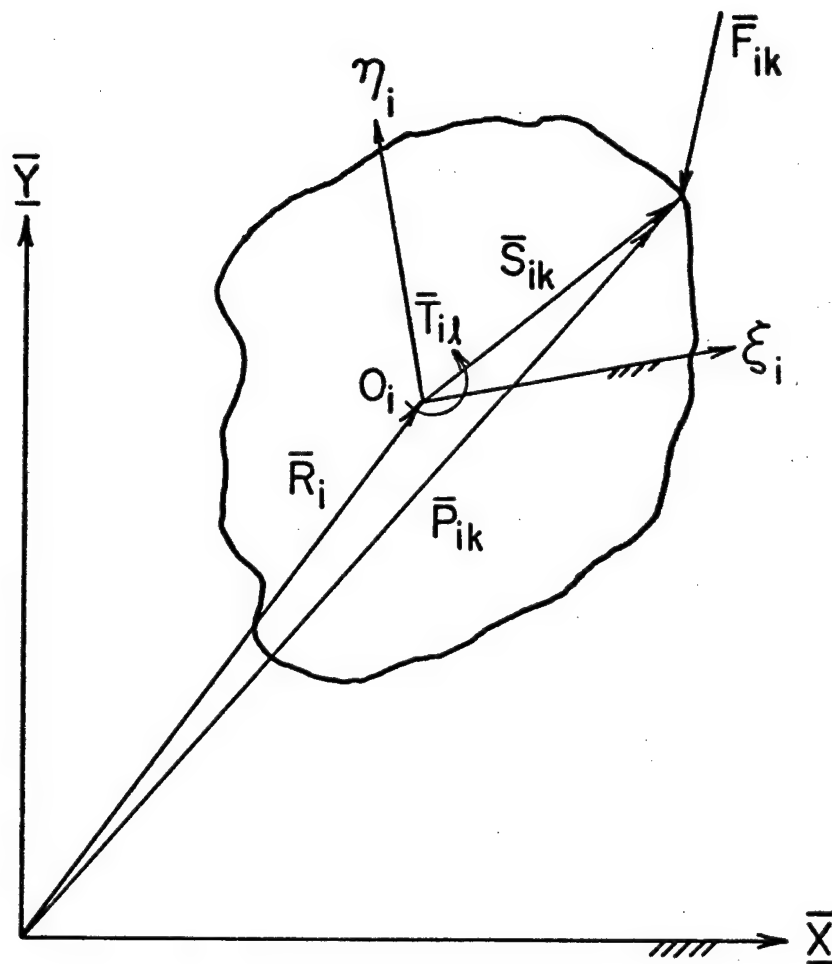
Figure 3.1 Force Acting on Body i

M_i = Total number of moments acting on body i

Since $\overline{R}_i$, $\overline{S}_{ik}$, and $\overline{\theta}_i$ are functions of the position state variables z, Eq. 3.1 can be written as

$$\delta w_i = \left\{ \sum_{k=1}^{N_i} \overline{F}_{ik} \cdot \left(\frac{\partial \overline{R}_i}{\partial z} + \frac{\partial \overline{S}_{ik}}{\partial z} \right) \delta z + \sum_{\ell=1}^{M_i} \overline{T}_{i\ell} \cdot \frac{\partial \overline{\theta}_i}{\partial z} \delta z \right\} \tag{3.2}$$

The virtual work for a system of n bodies can then be written as

$$\delta W = \sum_{i=1}^{n} \delta w_i \tag{3.3}$$

Since the state equations for position of Eq. 2.6 are a system of workless constraints, the principle of virtual work [23] requires that δW of Eq. 3.3 be zero, for all virtual displacements that are consistent with the constraints. These virtual displacments are all δz satisfying.

$$\delta \Phi = \left[\frac{\partial \overline{\Phi}}{\partial z} \right] \delta z = 0 \tag{3.4}$$

where $\Phi \equiv \Phi(z,b,\alpha)$.

Farkas Lemma [20] now guarantees the existence of a vector $\mu \in R^{3n}$ of multipliers such that

$$\delta W - \mu^T \delta \Phi = 0 \tag{3.5}$$

for all $\delta z \in R^{3n}$. Substituting from Eqs. 3.2, 3.3, and 3.4 into Eq. 3.5, one has

$$
\left\{ \sum_{i=1}^{n} \left\{ \sum_{k=1}^{N_i} \overline{F}_{ik} \cdot \left(\frac{\partial \overline{R}_i}{\partial z} + \frac{\partial \overline{S}_{ik}}{\partial z} \right) + \sum_{\ell=1}^{M_i} \overline{T}_{i\ell} \cdot \frac{\partial \overline{\theta}_i}{\partial z} \right\} - \mu^T \frac{\partial \Phi}{\partial z} \right\} \delta z = 0
$$

(3.6)

which must hold for all $\delta z \in R^{3n}$. Since δz is arbitrary in Eq. 3.6, each of its components can be varied independently, to obtain the matrix equation

$$
\sum_{i=1}^{n} \left[\sum_{k=1}^{N_i} \overline{F}_{ik} \cdot \left(\frac{\partial \overline{R}_i}{\partial z} + \frac{\partial \overline{S}_{ik}}{\partial z} \right) + \sum_{\ell=1}^{M_i} \overline{T}_{i\ell} \cdot \frac{\partial \overline{\theta}_i}{\partial z} \right]^T - \left(\frac{\partial \Phi}{\partial z} \right)^T \mu = 0
$$

(3.7)

Equation 3.7 can be rewritten in the form

$$
\left(\frac{\partial \Phi}{\partial z} \right)^T \mu = H
$$

(3.8)

where

$$
H = \sum_{i=1}^{n} \left\{ \sum_{k=1}^{N_i} \overline{F}_{ik} \cdot \left(\frac{\partial \overline{R}_i}{\partial z} + \frac{\partial \overline{S}_{ik}}{\partial z} \right) + \sum_{\ell=1}^{M_i} \overline{T}_{i\ell} \cdot \frac{\partial \overline{\theta}_i}{\partial z} \right\}^T
$$

(3.9)

Since the coefficient matrix of Eq. 3.8 is the transpose of the Jacobian matrix of Eq. 2.19, this linear system is guaranteed to have a unique solution. This Jacobian matrix, as stated in Section 2.2.3, has already been symbolically factored and stored. Solving Eq. 3.8 is thus the same as solving Eq. 2.19, but with a transposed coefficient matrix and a different right-hand side. The solution of Eq. 3.8 is thus very efficient.

3.2 Force Equations From Lagrange's
Equations of Motion

Lagrange's equations of motion for a dynamic system can be applied as force equations for kinematic systems. Considering Lagrange's equations for a general constrained mechanical system [23],

$$\frac{d}{dt}\left(\frac{\partial T}{\partial \dot{z}_k}\right) - \left(\frac{\partial T}{\partial z_k}\right) + \sum_{\ell=1}^{r} \mu_\ell \frac{\partial \Phi_\ell}{\partial z_k} = (Q_k)_{nc} + (Q_k)_c$$

$$k = 1,\ldots,3n \qquad (3.10)$$

where

  T = kinetic energy of the system

$(Q_k)_{nc}$ = nonconservative generalized force corresponding to the kth

    generalized coordinate

$(Q_k)_c$ = conservative generalized force corresponding to the kth

    generalized coordinate

  r = total number of constraints on the system, in the present

    context $r = 3n$

  μ = vector of time-dependent Lagrange multipliers

In this form, Lagrange's equations are a system of 3n equations in 3n z_k's and 3n μ_i's. The 3n equations of constraint have also to be considered along with Eq. 3.10, to solve for the 6n unknowns (3n z_k's + 3n μ_i's). However, since the 3n equations of constraint have already been solved for 3n z_k's, Eq. 3.10 has only 3n μ_i's as unknowns. The

generalized velocities and accelerations for the system have already
been determined. Hence, the first term in Eq. 3.10 is a known quantity.
Since the kinetic energy of the system does not directly depend on the
generalized coordinates, the second term in Eq. 3.10 is zero. Equation
3.10 can thus be rewritten as

$$\sum_{\ell=1}^{3n} \mu_\ell \left(\frac{\partial \Phi_\ell}{\partial z_k} \right) = (Q_k)_{nc} + (Q_k)_c - \frac{d}{dt} \left(\frac{\partial T}{\partial \dot{z}_k} \right), \qquad k = 1, \ldots, 3n$$

(3.11)

The right-hand side of Eq. 3.11 may be written as

$$(Q_k)_s = (Q_k)_{nc} + (Q_k)_c - \frac{d}{dt} \left(\frac{\partial T}{\partial \dot{z}_k} \right)$$ (3.12)

where

$(Q_k)_s$ is the total generalized forces corresponding to the gener-
ized coordinate z_k.

Using Eq. 3.12, Eq. 3.11 can be written as

$$\sum_{\ell=1}^{3n} \mu_\ell \frac{\partial \Phi_\ell}{\partial z_k} = (Q_k)_s, \qquad k = 1, \ldots, 3n$$ (3.13)

Expressing Eq. 3.13 as a matrix equation, gives

$$\left(\frac{\partial \Phi}{\partial z} \right)^T \mu = G$$ (3.14)

where

G is the vector of $(Q_k)_s$, $k = 1, \ldots, 3n$

The force equation obtained from the Lagrange equations of
motion, Eq. 3.14, and the equilibrium equation obtained from the

principle of virtual work, Eq. 3.8, are of the same form. However, the right side of Eq. 3.14 includes dynamic effects. These dynamic effects include D'Alembert's forces and moments and forces and torques due to spring dampers. For mechanisms being acted upon by static forces only, it is possible to show that the right side of Eq. 3.8 and 3.14 are equivalent.

The kinetic energy of the system can be written as

$$T = \sum_{k=1}^{3n} m_k (\dot{z}_k)^2 \tag{3.15}$$

where

m_k = mass of body i if

$\quad k = \{3i - 2, 3i - 1 \mid 1 \leqslant i \leqslant n\}$

$\quad$ = mass moment of inertia of body i if

$\quad k = 3i \ , \ 1 \leqslant i \leqslant n$

Substituting kinetic energy T from Eq. 3.15 into the third term of Eq. 3.11 gives

$$\frac{d}{dt}\left(\frac{\partial T}{\partial \dot{z}_k}\right) = \frac{d}{dt} \ m_k \dot{z}_k = m_k \ddot{z}_k \tag{3.16}$$

The third term in Eq. 3.11, depending on index k, is thus D'Alemberts force or moment. This term can be denoted by a generalized force term $(Q_k)_D$. The right side of Eq. 3.11 can thus be written as

$$(Q_k)_s = \{(Q_k)_{nc} + (Q_k)_c - (Q_k)_D\} \tag{3.17}$$

Consider the mechanical system being acted upon by a system of forces $\overline{F}_{ik}$ and moments $\overline{T}_{i\ell}$. The generalized forces due to this force system can be directly written as [24]

$$(Q_k)_F = \sum_{i=1}^{n} \left[\sum_{\ell=1}^{N_i} \overline{F}_{i\ell} \cdot \frac{\partial \overline{P}_{i\ell}}{\partial z_k} + \sum_{\ell=1}^{M_i} \overline{T}_{i\ell} \cdot \frac{\partial \overline{\theta}_i}{\partial z_k} \right] \qquad (3.18)$$

where $\overline{P}_{i\ell}$ is the vector locating the point of application of force $\overline{F}_{i\ell}$ in the global reference frame.

Since the generalized coordinates being considered in Eq. 3.11 are the same as those in Eq. 3.18, the corresponding generalized forces can be equated; i.e.,

$$(Q_k)_S = (Q_k)_F - (Q_k)_D \qquad (3.19)$$

From Fig. 3.1, $\overline{P}_{i\ell}$ can be denoted as

$$\overline{P}_{i\ell} = \overline{R}_i + \overline{S}_{i\ell} \qquad (3.20)$$

Substituting for the right side of Eq. 3.19 from Eq. 3.18 gives

$$(Q_k)_S = \sum_{i=1}^{n} \left[\sum_{\ell=1}^{N_i} \overline{F}_{i\ell} \cdot \left(\frac{\partial(\overline{R}_i + \overline{S}_{i\ell})}{\partial z_k} \right) + \sum_{\ell=1}^{M_i} \overline{T}_{i\ell} \cdot \frac{\partial \overline{\theta}_i}{\partial z_k} \right] - (Q_k)_D \qquad (3.21)$$

Writing the above equation in vector form, one has

$$G = \sum_{i=1}^{n} \left[\sum_{\ell=1}^{N_i} \overline{F}_{i\ell} \cdot \left(\frac{\partial(\overline{R}_i + \overline{S}_{i\ell})}{\partial z} \right) + \sum_{\ell=1}^{M_i} \overline{T}_{i\ell} \cdot \frac{\partial \overline{\theta}_i}{\partial z} \right] - (\overline{Q})_D \qquad (3.22)$$

By directly comparing Eqs. 3.9 and 3.22, it can be seen that the right sides of Eqs. 3.8 and 3.14 differ by the term $(\overline{Q})_D$. Since $(\overline{Q})_D$ corresponds to the D'Alembert forces or moments, for static mechanisms, Eqs. 3.8 and 3.14 are completely equivalent. For mechanisms with dynamic effects, however, only Eq. 3.14 is valid.

3.3 Relating Lagrange Multipliers to Joint Reactions

The solution of Eq. 3.14 is the vector of Lagrange multipliers μ. To determine joint reactions, and the subsequent forces in the members, it is necessary to relate these Lagrange multipliers to the joint reaction forces. A method used in Ref. 13 will be used here to develop relationships between the Lagrange multipliers and joint reaction forces.

Consider a mechanism with n bodies and ℓ independent joints, with the state equations for position given by Eq. 2.6. For a typical joint in the mechanism, the equations of constraint are

$$\phi_r = 0$$

$$\phi_{r+1} = 0 \tag{3.23}$$

In differential form, Eq. 3.23 can be written as

$$\delta\phi_r = \sum_{i=1}^{3n} \frac{\partial\phi_r}{\partial z_i} \delta z_i$$

$$\delta\phi_{r+1} = \sum_{i=1}^{3n} \frac{\partial\phi_{r+1}}{\partial z_i} \delta z_i \tag{3.24}$$

If this joint were to be 'broken', the equations of constraint of Eq. 3.23 would no longer hold. However, if the defects (violations) in constraint equations are given by δd_r and δd_{r+1}, respectively, then the following conditions hold

$$\delta\phi_r + \delta d_r = 0$$

$$\delta\phi_{r+1} + \delta d_{r+1} = 0 \tag{3.25}$$

The displacements δd_r and δd_{r+1} are functions of the generalized coordinates and can be written, s

$$\delta d_r = - \sum_{i=1}^{3n} \frac{\partial \phi_r}{\partial z_i} \delta z_i \equiv \sum_{i=1}^{3n} c_{i,r} \delta z_i \qquad (3.26)$$

$$\delta d_{r+1} = - \sum_{i=1}^{3n} \frac{\partial \phi_{r+1}}{\partial z_i} \delta z_i \equiv \sum_{i=1}^{3n} c_{i,r+1} \delta z_i \qquad (3.27)$$

where

$c_{i,r}$ and $c_{i,r+1}$ are functions of the generalized coordinates.

The virtual work of the joint reactions, R_r and R_{r+1} in the direction of d_r and d_{r+1}, respectively, can be written as

$$\delta W_k = R_r \delta d_r + R_{r+1} \delta d_{r+1} \qquad (3.28)$$

where

Joint reactions R_r and R_{r+1} can be either forces or moments, and k is the number of the joint that has been 'broken'.

If each joint and driving constraint in the system is 'broken', the virtual work of the reaction forces is given by

$$\delta W_R = \sum_{k=1}^{\ell} \delta w_k + \sum_{p=2\ell+1}^{2\ell+m} R_p \delta d_p = \sum_{r=1}^{3n} R_r \delta d_r \qquad (3.29)$$

where p is the index of the driving constraint. Using Eq. 3.25, Eq. 3.29 can be written as

$$\delta W_R = -\sum_{r=1}^{3n} R_r \delta \phi_r \qquad (3.30)$$

Substituting from Eq. 3.24,

$$\delta W_R = - \sum_{i=1}^{3n} \sum_{r=1}^{3n} R_r \frac{\partial \phi_r}{\partial z_i} \delta z_i \qquad (3.31)$$

The virtual work of the external and dynamic forces can be expressed in the form

$$\delta W_E = \sum_{i=1}^{3n} (Q_i)_S \, \delta z_i \tag{3.32}$$

where $(Q_i)_S$ is the generalized force associated with the ith generalized coordinate. Since the joints are considered broken, the equations of constraint of Eq. 2.6 can be ignored. Hence, δz_i is arbitrary and independent. Setting the total virtual work to zero, $\delta W_R + \delta W_E = 0$, for all δz gives

$$(Q_i)_S = \sum_{r=1}^{3n} R_r \frac{\partial \phi_r}{\partial z_i} \quad , \qquad i = 1,\ldots,3n \tag{3.33}$$

In matrix form, Eq. 3.33 becomes

$$\left[\frac{\partial \Phi}{\partial z}\right]^T \overline{R} = G \tag{3.34}$$

where

$\overline{R}$ = vector of reaction forces R_r and

G = vector of generalized forces

Comparing Eqs. 3.34 and 3.14, it can be concluded that

$$R_i = \mu_i \tag{3.35}$$

Thus, the Lagrange multipliers, computed as a solution of Eq. 3.14, are the reaction forces or moments in the joints or due to the driving constraints. The definition of joint reaction forces R_i, however, depends upon the definition of the constraint defects δd_i.

Consider now the two typical joints described in Chapter 2. The joint reactions in the revolute joint are the forces in the global X

and Y direction respectively. For the translational joint, the joint reactions are the moment in the joint and a force acting normal to the line of translation. It still needs to be shown that the vector of reactions $\overline{R}$ actually represents the above-mentioned reaction forces.

3.3.1 Reaction Forces in Revolute Joint

Considering a revolute joint k that connects body i and body j, Eqs. 2.7 can be rewritten as

$$(\overline{r}_p)_k = \left(\overline{R}_j + \overline{r}_{ji} - \overline{R}_i - \overline{r}_{ij} \right)_k \tag{3.36}$$

The vector $\overline{r}_p$ can be written in terms of its x and y components, r_{p_x} and r_{p_y} as

$$(\overline{r}_p)_k = \left[r_{p_x} \quad r_{p_y} \right]^T_k$$

To derive the equations of constraint for the revolute joint, the condition $\overline{r}_p = 0$ was used to get

$$(\overline{r}_p)_k = \begin{bmatrix} r_{p_x} \\ r_{p_y} \end{bmatrix}_k = - \begin{bmatrix} \phi_x \\ \phi_y \end{bmatrix}_k = 0 \tag{3.37}$$

In differential form, when $\delta\overline{r}_p \neq 0$,

$$\begin{bmatrix} -\delta r_{p_x} \\ -\delta r_{p_y} \end{bmatrix}_k = \begin{bmatrix} \delta\phi_x \\ \delta\phi_y \end{bmatrix}_k \tag{3.38}$$

Equation 3.38 implies that for a 'broken' revolute joint, the variation of the x and y constraint equations represents the negative of the defect along the X and Y axes, respectively. From Eqs. 3.24 and 3.38,

$$\delta d_r = (\delta r_{p_x})_k \qquad (3.39)$$

$$\delta d_{r+1} = (\delta r_{p_y})_k \qquad (3.40)$$

where index r corresponds to the index of first constraint equation, due to revolute joint k.

From Eqs. 3.39 and 3.40, it can be concluded that the Lagrange multipliers corresponding to the two equations of constraint of a revolute joint are the x and y reactions in the revolute joint.

3.3.2 Reaction Forces in Translational Joint

To derive the reaction forces for the translational joint, a variation of the procedure derived in Section 3.3 is used. Since the two equations of constraint for any joint are independent, instead of breaking one joint at a time, only one constraint condition for the joint is broken at a time. The unbroken constraint is thus still valid.

Consider the second equation of constraint for the translational joint, given by Eq. 2.15 as

$$\phi_\theta = (U_i - x_i)(V_j - y_j) - (V_i - y_i)(U_j - x_j)$$

In differential form, this is

$$\delta\phi_\theta = (\delta U_i - \delta x_i)(V_j - y_j) + (U_i - x_i)(\delta V_j - \delta y_j)$$

$$- (\delta V_i - \delta y_i)(U_j - x_j) - (V_i - y_i)(\delta U_j - \delta x_j) \qquad (3.41)$$

Substituting the differential form of U_i, U_j, V_i, and V_j from Eq. 2.14 into Eq. 3.41 gives

$$\delta\phi_\theta = \{-(\xi_{ij} \sin\theta_i + \eta_{ij} \cos\theta_i)(\xi_{ji} \sin\theta_j + \eta_{ji} \cos\theta_j)$$

$$-(\xi_{ij} \cos\theta_i - \eta_{ij} \sin\theta_i)(\xi_{ji} \cos\theta_j - \eta_{ji} \sin\theta_j)\}$$

$$\times (\delta\theta_i - \delta\theta_j) \qquad (3.42)$$

Equation 3.42 can be written as

$$\delta\phi_\theta = c_{\theta_{ij}} (\delta\theta_i - \delta\theta_j) \qquad (3.43)$$

where $c_{\theta_{ij}}$ represents the term in curly brackets in Eq. 3.42.

Thus the condition $\phi_\theta = 0$ constrains relative rotation of bodies i and j.

With

$$\delta\phi_\theta + \delta d_\theta = 0$$

as in Eq. 3.25,

$$\delta d_\theta = - c_{\theta_{ij}} (\delta\theta_i - \delta\theta_j)$$

which is proportional to a virtual relative rotation of bodies i and j. This shows that

$$\mu_\theta \delta d_\theta = -\mu_\theta c_{\theta_{ij}} (\delta\theta_i - \delta\theta_j)$$

so $\mu_\theta c_{\theta_{ij}}$ is the reaction torque acting between bodies i and j, due to a translational joint.

Consider now the first equation of constraint for the translational joint, given by Eq. 2.13 as

$$\phi_n = (U_i - x_i)(U_i - U_j) + (V_i - y_i)(V_i - V_j)$$

In differential form, this is

$$\delta\phi_n = (\delta U_i - \delta x_i)(U_i - U_j) + (U_i - x_i)(\delta U_i - \delta U_j)$$

$$- (\delta V_i - \delta y_i)(V_i - V_j) + (V_i - y_i)(\delta V_i - \delta V_j) \qquad (3.45)$$

Substituting the differential forms for U_i, V_j, V_i and V_j from Eq. 2.14 into Eq. 3.45 gives

$$\delta\phi_n = \left[-(V_i - y_i)\delta\theta_i\right](x_i - x_j) + \left[(U_i - x_i)\delta\theta_j\right](y_i - y_j)$$

$$+ \left[(U_i - x_i)\right](\delta x_i - \delta x_j) + \left[V_i - y_i\right](\delta y_i - \delta y_j)$$

$$- (V_i - y_i)(-\xi_{ji}\cos\theta_j + \eta_{ji}\sin\theta_j)\delta\theta_i$$

$$- (\xi_{ij}\cos\theta_i - \eta_{ij}\sin\theta_i)(\xi_{ij}\sin\theta_i + \eta_{ij}\cos\theta_i)\delta\theta_i$$

$$+ (U_i - x_i)(\xi_{ij}\sin\theta_i + \eta_{ij}\cos\theta_i)\delta\theta_j$$

$$- (\xi_{ij}\sin\theta_i + \eta_{ij}\cos\theta_i)(\xi_{ji}\cos\theta_j - \eta_{ji}\sin\theta_j)\delta\theta_j$$

The above expression can further be simplified to

$$\delta\phi_n = \left[-(V_i - y_i)\delta\theta_i\right](x_i - x_j) + \left[(U_i - x_i)\delta\theta_j\right](y_i - y_j)$$

$$+ \left[U_i - x_i\right](\delta x_i - \delta x_j) + \left[V_i - y_i\right](\delta y_i - \delta y_j)$$

$$+ \left\{(\xi_{ij}\sin\theta_i + \eta_{ij}\cos\theta_i)(\xi_{ji}\cos\theta_j - \eta_{ji}\sin\theta_j)\right.$$

$$\left. - (\xi_{ij}\cos\theta_i - \eta_{ij}\sin\theta_i)(\xi_{ij}\sin\theta_i + \eta_{ij}\cos\theta_i)\right\}(\delta\theta_i - \delta\theta_j)$$

$$(3.46)$$

Since each of the two equations of constraint for this joint are being 'broken' one at a time, the second equation of constraint for this joint, Eq. 2.16, is valid here. From Eq. 3.43, this implies

$$\delta\phi_\theta = c_{\theta_{ij}} (\delta\theta_i - \delta\theta_j) = 0 \tag{3.47}$$

Coefficient $c_{\theta_{ij}}$ has to be nonzero to get a nontrivial constraint equation. Equation 3.27 thus implies

$$(\delta\theta_i - \delta\theta_j) = 0 \tag{3.48}$$

Substituting Eq. 3.48 into Eq. 3.46 gives

$$\delta\phi_n = \left[-(V_i - y_i)\delta\theta_i\right](x_i - x_j) + \left[(U_i - x_i)\delta\theta_j\right](y_i - y_j)$$

$$+ \left[U_i - x_i\right](\delta x_i - \delta x_j) + \left[V_i - y_i\right](\delta y_i - \delta y_j) \tag{3.49}$$

To develop an interpretation of Eq. 3.49, consider Fig. 2.3 again. Write a unit vector $\bar{n}$ along $\bar{r}_{ij}$ as

$$\bar{n} = \frac{1}{|\bar{r}_{ij}|} \left\{(U_i - x_i)\,\bar{I} + (V_i - y_i)\,\bar{J}\right\} \tag{3.50}$$

Since ϕ_θ is still a valid constraint, $\bar{n}$ is also parallel to $\bar{r}_{ji}$. The projection of the position vectors of the body-fixed coordinate systems of bodies i and j along $\bar{n}$ can be expressed by n_i and n_j, respectively as,

$$n_i = \bar{n} \cdot \bar{R}_i \tag{3.51}$$

$$n_j = \bar{n} \cdot \bar{R}_j \tag{3.52}$$

Denote $\bar{n}$ as

$$\bar{n} = n_1 \bar{I} + n_2 \bar{J} \tag{3.53}$$

where

$$n_1 = (U_i - x_i)/|\overline{r}_{ij}|$$

$$n_2 = (V_i - y_i)/|\overline{r}_{ij}|$$

In differential form, Eqs. 3.51 and 3.52 can be written as

$$\delta n_i = \delta n_1 x_i + n_1 \delta x_i + \delta n_2 y_i + n_2 \delta y_i \tag{3.54}$$

$$\delta n_j = \delta n_1 x_j + n_1 \delta x_j + \delta n_2 y_j + n_2 \delta y_j \tag{3.55}$$

The virtual displacement of body i relative to body j along the direction of vector $\overline{n}$ can be expressed as

$$\delta n_i - \delta n_j = \delta n_1 (x_i - x_j) + \delta n_2 (y_i - y_j)$$

$$+ n_1 (\delta x_i - \delta x_j) + n_2 (\delta y_i - \delta y_j) \tag{3.56}$$

Observing that $|\overline{r}_{ij}|$ is invariant under a rotation, the differential forms of n_1 and n_2 can be written as

$$\delta n_1 = - \frac{(V_i - y_i)}{|\overline{r}_{ij}|} \delta \theta_i \tag{3.57}$$

$$\delta n_2 = - \frac{(U_i - x_i)}{|\overline{r}_{ij}|} \delta \theta_i \tag{3.58}$$

Substituting δn_1, δn_2 and $\delta \theta_i$ from Eqs. 3.57, 3.58 and 3.48, respectively, into Eq. 3.56 gives

$$\delta n_i - \delta n_j = \frac{1}{|\overline{r}_{ij}|} \left\{ \left[-(V_i - y_i) \delta \theta_i \right](x_i - x_j) \right.$$

$$+ \left[(U_i - x_i) \delta \theta_j \right](y_i - y_j) + \left[U_i - x_i \right](\delta x_i - \delta x_j)$$

$$+ \left[V_i - y_i \right](\delta y_i - \delta y_j) \right\} \tag{3.59}$$

Comparing Eqs. 3.49 and 3.59 gives

$$\delta \phi_n = |\overline{r}_{ij}|(\delta n_i - \delta n_j) \tag{3.60}$$

Rewrite Eq. 3.60 as

$$\delta \phi_n = c_{n_{ij}} (\delta n_i - \delta n_j) \tag{3.61}$$

where $c_{n_{ij}} = |\overline{r}_{ij}|$. Thus the condition $\phi_n = 0$ constraint relative translation of bodies i and j in the direction $\overline{n}$.

With

$$\delta \phi_n + \delta d_n = 0$$

as in Eq. 3.25,

$$\delta d_n = - c_{n_{ij}} (\delta n_i - \delta n_j)$$

is proportional to a normal virtual relative displacement of bodies i and j. This shows that

$$-\mu_n \delta d_n = -\mu_n c_{n_{ij}} (\delta n_i - \delta n_j)$$

so $\mu_n c_{n_{ij}}$ is the normal reaction force acting between bodies i and j, due to a translational joint.

CHAPTER 4

OPTIMAL DESIGN OF MECHANISMS

4.1 Introduction

Chapters 2 and 3 provide the theory necessary to compute the kinematics of the mechanism and the forces acting on the links of the mechanism. It should, therefore, be possible to put design constraints (bounds) directly on these variables or on functions of these variables. Also, it should be possible to make extreme any of the state variables or their functions, subject to constraints.

Most extreme algorithms used require that explicit derivatives, with respect to design variables, of the cost and constraint functions be provided. Computing derivatives of functions involving only design variables is easy. However, for functions involving state variables, the dependence on design arises indirectly, through the state equation. Derivative computation of such functions is thus not as simple as that for explicit functions of design variables. An adjoint variable technique that has been used for design sensitivity analysis of structural system [20], is used in this chapter for design sensitivity analysis of mechanisms.

4.2 Statement of the Optimal Design Problem

4.2.1 Statement of Continuous Optimization Problem

A general class of optimal design problems can be stated as:

Find a design $b \in R^S$ to minimize the cost function

$$\psi_0 \equiv \psi_0(b) \tag{4.1}$$

subject to State Equations;

(A.1) Position State Equation of Eq. 2.6

$$\Phi(z,b,\alpha) = 0 \tag{4.2}$$

(A.2) Velocity State Equation of Eq. 2.23

$$\left[\frac{\partial \Phi(z,b,\alpha)}{\partial z}\right] \dot{z} = -\frac{\partial \Phi(\dot{z},b,\alpha)}{\partial \alpha} \dot{\alpha} \tag{4.3}$$

(A.3) Acceleration State Equation of Eq. 2.27

$$\left[\frac{\partial \Phi(z,b,\alpha)}{\partial z}\right] \ddot{z} = -\left[\frac{\partial}{\partial z}\left[\frac{\partial \Phi(z,b,\alpha)}{\partial z} \dot{z}\right] \dot{z}\right] - \Omega$$

(A.4) Force Equation of Eq. 3.14

$$\frac{\partial \Phi(z,b,\alpha)}{\partial z}^T \mu = G \tag{4.5}$$

and Composite Design Constraints;

(B.1) Inequality Constraints

$$\psi_i(z,\dot{z},\ddot{z},\mu,b) \le 0 , \qquad i = 1,\ldots,p \tag{4.6}$$

(B.2) Equality Constraints

$$\psi_i(z,\dot{z},\ddot{z},\mu,b) = 0 , \qquad i = p + 1,\ldots,p + q \tag{4.7}$$

Equations 4.1 to 4.7 define a general optimal design problem. Any type of design constraint can be treated in this formulation, as long as it can be put in a form such as Eqs. 4.6 or 4.7. The representation of the cost function in the form of Eq. 4.1 does not restrict the technique from being applied to cost functions involving state variables. An upper bound technique [20] that is used in such cases is now illustrated for a general function $\hat{\psi}_0(z,\dot{z},\ddot{z},\mu,b)$, the maximum value of which is

required to be minimized, over a specified range of input parameters α. Thus,

$$\min_{b} \hat{\psi}_0 \equiv \min_{b} \left\{ \max_{\alpha} \hat{\psi}_0(z,\dot{z},\ddot{z},\mu,b) \right\} \tag{4.8}$$

The above formulation of the cost function is natural for kinematic optimization. Since state variables take on different values over the entire range of input parameters, it is natural to minimize the maximum value of functions of these variables.

Equation 4.8 represents a mini-max problem [20] and is not simple to deal with directly. A scheme commonly employed is to introduce an artificial design variable b_{S+1} to be an upper bound of $\hat{\psi}_0(z,\dot{z},\ddot{z},\mu,b)$. Therefore, the minimization problem in Eq. 4.8 can be written as

$$\min \psi_0 \equiv b_{S+1} \tag{4.9}$$

subject to the additional constraints

$$(i) \quad \psi_1(z,\dot{z},\ddot{z},\mu,b) \equiv \left\{ \max_{\alpha} \hat{\psi}_0(z,\dot{z},\ddot{z},\mu,b) \right\} - b_{S+1} \leq 0 \tag{4.10}$$

(ii) State Equations and other design constraints.
The minimization problem, as stated in Eqs. 4.9 and 4.10, amounts to generating a minimizing sequence of upper bounds of the function $\hat{\psi}_0$.

Composite design constraints in the form of Eqs. 4.6 and 4.7 are required to hold over the entire range of specified input parameters. Such constraints are called parametric constraints. Techniques for making cost functions extreme which are subject to parametric constraints have been developed earlier [25]. Since these techniques require a con- siderable amount of additional computation, a simpler approximate tech- nique is resorted to. The range of input parameters α is discretized

into a set of grid points α^j, $j = 1,\ldots,\tau$. The composite design constraints are then required to hold at every point on this grid.

4.2.2 Statement of Discretized Optimal Design Problem

The optimal design problem, with a grid imposed on the range of the input parameters, can be stated as follows:

Find a design b R^s to minimize the cost function

$$\psi_0 \equiv \psi_0(b) \tag{4.11}$$

subject to State Equations;

(A.1) Position State Equations of Eq. 2.6

$$\Phi(z^j,b,\alpha^j) = 0 \quad , \qquad j = 1,\ldots,\tau \tag{4.12}$$

where τ = number of grid points on the range of the input parameters.

(A.2) Velocity State Equation of Eq. 2.23

$$\left[\frac{\partial\Phi(z^j,b,\alpha^j)}{\partial z}\right]\dot{z}^j = -\frac{\partial\Phi}{\partial\alpha}(z^j,b,\alpha^j)\dot{\alpha}^j \quad , \qquad j = 1,\ldots,\tau \tag{4.13}$$

(A.3) Acceleration State Equation of Eq. 2.27

$$\left[\frac{\partial\Phi(z^j,b,\alpha^j)}{\partial z}\right]\ddot{z}^j = -\frac{\partial}{\partial z}\left[\frac{\partial\Phi(z^j,b,\alpha^j)}{\partial z}\dot{z}^j\right]\dot{z}^j - \Omega^j \quad , \qquad j = 1,\ldots,\tau$$

$$\tag{4.14}$$

(A.4) Force Equation of Eq. 3.14

$$\left[\frac{\partial\Phi(z^j,b,\alpha^j)}{\partial z}\right]^T \mu^j = G^j \quad , \qquad j = 1,\ldots,\tau \tag{4.15}$$

and Composite Design Constraints;

(B.1) Inequality Constraints

$$\psi_i(z^j,\dot{z}^j,\ddot{z}^j,\mu^j,b) < 0, \quad i = 1,\ldots,p, \quad j = 1,\ldots,\tau \tag{4.16}$$

(B.2) Equality Constraints

$$\psi_i(z^j, \dot{z}^j, \ddot{z}^j, \mu^j, b) = 0, \quad i = p+1, \ldots, p+q, \quad j = 1, \ldots, \tau$$

(4.17)

4.3 Design Sensitivity Analysis

As noted in the introduction to this chapter, all design optimization algorithms require that derivatives of cost and constraint functions, with respect to design variables, be provided. Having stated the optimal design problem, it is now possible to proceed to deriving the derivatives of the cost and constraint functions. This derivation is restricted to the discretized optimal design problem.

The first variation of the cost function of Eq. 4.11 can be written simply as

$$\delta\psi_0 \equiv \frac{\partial\psi_0(b)}{\partial b} \, \delta b = \ell^{0^T} \delta b$$

(4.18)

Since the cost function can always be reduced to a function of design variables by the method explained in Section 4.2.1, the sensitivity of the cost function can very simply be written in the form of Eq. 4.18.

The first variation of the composite design constraint can be written as

$$\delta\psi^{ij^T} = \left\{ \left(\frac{\partial\psi_i}{\partial z} \right) \delta z + \left(\frac{\partial\psi_i}{\partial \dot{z}} \right) \delta\dot{z} + \left(\frac{\partial\psi_i}{\partial \ddot{z}} \right) \delta\ddot{z} + \left(\frac{\partial\psi_i}{\partial \mu} \right) \delta\mu \right.$$
$$\left. + \left(\frac{\partial\psi_i}{\partial b} \right) \delta b \right\}_j \quad , \quad i = 1, \ldots, p+q \ , \quad j = 1, \ldots, \tau$$

(4.19)

Since Eq. 4.19 is valid for equality and inequality constraints, the index i runs from 1 to (p+q). In vector form, Eq. 4.19 can be rewritten as

$$\delta\psi^{ij} = \left[\left(\frac{\partial\psi_i}{\partial z}\right) \bigg| \left(\frac{\partial\psi_i}{\partial \dot{z}}\right) \bigg| \left(\frac{\partial\psi_i}{\partial \ddot{z}}\right) \bigg| \left(\frac{\partial\psi_i}{\partial \mu}\right)\right]_j \begin{bmatrix} \delta z \\ \hline \delta\dot{z} \\ \hline \delta\ddot{z} \\ \hline \delta\mu \end{bmatrix}_j + \left(\frac{\partial\psi_i}{\partial b}\right)_j \delta b$$

$$i = 1,\ldots,p+q , \qquad j = 1,\ldots,\tau \qquad (4.20)$$

Since the state variables are functions of the design, it is required that the variations of the state variables in Eq. 4.20 be written in terms of variations in design. The objective is then to write Eq. 4.20 as

$$\delta\psi^{ij} \equiv \ell^{ij^T} \delta b \qquad (4.21)$$

where ℓ^{ij} is the design sensitivity vector of the ith constraint at the jth grid point α^j.

Observing that the state equations couple the design and state variables, the first variation of the four state equations, Eqs. 4.12, 4.13, 4.14, and 4.15, can be written as

$$\left\{\left(\frac{\partial\Phi}{\partial z}\right) \delta z + \left(\frac{\partial\Phi}{\partial b}\right) \delta b\right\}_j = 0 \qquad (4.22)$$

$$\left\{ \frac{\partial}{\partial z} \left[\left(\frac{\partial \Phi}{\partial z}\right) \dot{z} \right] \delta z + \frac{\partial}{\partial b} \left[\left(\frac{\partial \Phi}{\partial z}\right) \dot{z} \right] \delta b + \left(\frac{\partial \Phi}{\partial z}\right) \dot{\delta z} \right\}_j$$

$$= \left\{ - \frac{\partial}{\partial z} \left[\frac{\partial \Phi}{\partial \alpha} \dot{\alpha} \right] \delta z - \frac{\partial}{\partial b} \left[\frac{\partial \Phi}{\partial \alpha} \dot{\alpha} \right] \delta b \right\}_j \qquad (4.23)$$

$$\left\{ \frac{\partial}{\partial z} \left[\left(\frac{\partial \Phi}{\partial z}\right) \ddot{z} \right] \delta z + \left(\frac{\partial \Phi}{\partial z}\right) \ddot{\delta z} + \frac{\partial}{\partial b} \left[\left(\frac{\partial \Phi}{\partial z}\right) \ddot{z} \right] \delta b \right\}_j$$

$$= \left\{ - \frac{\partial}{\partial z} \left[\frac{\partial}{\partial z} \left[\left(\frac{\partial \Phi}{\partial z}\right) \dot{z} \right] \dot{z} \right] \delta z - \frac{\partial}{\partial \dot{z}} \left[\frac{\partial}{\partial z} \left[\left(\frac{\partial \Phi}{\partial z}\right) \dot{z} \right] \dot{z} \right] \dot{\delta z} \right.$$

$$\left. - \frac{\partial}{\partial b} \left[\frac{\partial}{\partial z} \left[\left(\frac{\partial \Phi}{\partial z}\right) \dot{z} \right] \dot{z} \right] \delta b - \left(\frac{\partial \Omega}{\partial z}\right) \delta z - \left(\frac{\partial \Omega}{\partial b}\right) \delta b \right\}_j \qquad (4.24)$$

$$\left\{ \frac{\partial}{\partial z} \left[\left(\frac{\partial \Phi}{\partial z}\right)^T \right] \mu \quad \delta z + \frac{\partial}{\partial z} \left[\left(\frac{\partial \Phi}{\partial b}\right)^T \mu \right] \delta b + \left(\frac{\partial \Phi}{\partial z}\right)^T \delta \mu \right\}_j$$

$$\qquad (4.25)$$

$$= \left\{ \left(\frac{\partial G}{\partial z}\right) \delta z + \left(\frac{\partial G}{\partial \dot{z}}\right) \dot{\delta z} + \left(\frac{\partial G}{\partial \ddot{z}}\right) \ddot{\delta z} + \left(\frac{\partial G}{\partial b}\right) \delta b \right\}_j$$

Moving all terms in Eqs. 4.22 through 4.25 involving δb to the right side, this system of equations can be written in matrix form as

$$
\begin{bmatrix}
-\left(\dfrac{\partial \Phi}{\partial b}\right) \\[6pt]
-\dfrac{\partial}{\partial b}\left[z\cdot\left(\dfrac{\partial \Phi}{\partial z}\right)\right] \\[6pt]
-\dfrac{\partial}{\partial b}\left[\alpha\cdot\dfrac{\partial \Phi}{\partial z}\right] \\[6pt]
-\dfrac{\partial}{\partial b}\left[\dfrac{\partial}{\partial z}\left[z\cdot\left(\dfrac{\partial \Phi}{\partial z}\right)\right]\right] \\[6pt]
-\dfrac{\partial}{\partial b}\left[\dfrac{\partial}{\partial z}\left(\dfrac{\partial \Phi}{\partial z}\right)\cdot z\right]-\left(\dfrac{\partial \Omega}{\partial b}\right) \\[6pt]
+\dfrac{\partial}{\partial b}\left[\dfrac{\partial}{\partial z}\left(\dfrac{\partial \Phi}{\partial z}\right)^{T}u\right]+\left(\dfrac{\partial G}{\partial b}\right)
\end{bmatrix}
\boxed{\,\delta b\,}
$$

$$=\quad
\begin{bmatrix}\ \delta z\ \mid\ \delta \dot z\ \mid\ \delta \ddot z\ \mid\ \delta u\ \end{bmatrix}
$$

$$
\begin{bmatrix}
\left(\dfrac{\partial \Phi}{\partial z}\right) & 0 & 0 & 0 \\[8pt]
\dfrac{\partial}{\partial z}\left[z\cdot\left(\dfrac{\partial \Phi}{\partial z}\right)\right]+ & 0 & 0 & 0 \\[8pt]
\dfrac{\partial}{\partial z}\left[\alpha\cdot\dfrac{\partial \Phi}{\partial z}\right] & \left(\dfrac{\partial \Phi}{\partial z}\right) & 0 & 0 \\[8pt]
\dfrac{\partial}{\partial z}\left[\dfrac{\partial}{\partial z}\left[z\cdot\left(\dfrac{\partial \Phi}{\partial z}\right)\right]\right]+\left(\dfrac{\partial \Omega}{\partial z}\right) & 0 & \left(\dfrac{\partial \Phi}{\partial z}\right) & 0 \\[8pt]
\dfrac{\partial}{\partial \dot z}\left[\dfrac{\partial}{\partial z}\left[\left(\dfrac{\partial \Phi}{\partial z}\right)\cdot z\right]\right]+ & -\left(\dfrac{\partial \Omega}{\partial \ddot z}\right) & -\left(\dfrac{\partial G}{\partial \dot z}\right) & \left(\dfrac{\partial \Phi}{\partial z}\right)^{T} \\[8pt]
\dfrac{\partial}{\partial z}\left[\left(\dfrac{\partial \Phi}{\partial z}\right)^{T}u\right]-\left(\dfrac{\partial G}{\partial z}\right) & -\left(\dfrac{\partial G}{\partial \dot z}\right) & &
\end{bmatrix}
$$

$$\tag{4.26}$$

49

Equations 4.26 can be symbolically written as

$$A(z^j, \dot{z}^j, \ddot{z}^j, \mu^j, b)\, \delta U^j = B(z^j, \dot{z}^j, \ddot{z}^j, \mu^j, b)\, \delta b \qquad (4.27)$$

where A represents the coefficient matrix on the left-hand side of Eq. 4.26, B represents the coefficient matrix on the right-hand side of Eq. 4.26, and

$$U^{j^T} = \begin{bmatrix} z^T & | & \dot{z}^T & | & \ddot{z}^T & | & \mu^T \end{bmatrix}^T_j$$

The variation of the composite vector of state variables can be solved from Eq. 4.27 as

$$\delta U^j = (A^j)^{-1} B^j\, \delta b \qquad (4.28)$$

where

$$A^j \equiv A(z^j, \dot{z}^j, \ddot{z}^j, \mu^j, b)$$

$$B^j \equiv B(z^j, \dot{z}^j, \ddot{z}^j, \mu^j, b)$$

In deducing Eq. 4.28 from Eq. 4.27, it is required that the matrix A^j be invertible. The existence of such an inverse is proved in Appendix A.

Equation 4.28 expresses the variation of state variables in terms of variations in the design variables. Substituting δU^j from Eq. 4.28 into Eq. 4.20 gives

$$\delta \psi^{ij} = \left[\left(\frac{\partial \psi_i}{\partial z}\right) \Big| \left(\frac{\partial \psi_i}{\partial \dot{z}}\right) \Big| \left(\frac{\partial \psi_i}{\partial \ddot{z}}\right) \Big| \left(\frac{\partial \psi_i}{\partial \mu}\right)\right]_j (A^j)^{-1} B^j\, \delta b + \left(\frac{\partial \psi_i}{\partial b}\right)_j \delta b$$

$$(4.29)$$

To avoid calculation of $(A^j)^{-1}$, the product of the row vector of constraint derivatives and $(A^j)^{-1}$ is denoted by a composite adjoint vector Λ^{ij^T}, i.e.,

$$\Lambda^{ij^T} = \left[\frac{\partial \psi_i}{\partial z} \;\middle|\; \frac{\partial \psi_i}{\partial \dot{z}} \;\middle|\; \frac{\partial \psi_i}{\partial \ddot{z}} \;\middle|\; \frac{\partial \psi_i}{\partial \mu} \right]_j (A^j)^{-1} \tag{4.30}$$

Equation 4.30 can be rewritten as

$$(A^j)^T \Lambda^{ij} = \left[\left(\frac{\partial \psi_i}{\partial z}\right)^T \;\middle|\; \left(\frac{\partial \psi_i}{\partial \dot{z}}\right)^T \;\middle|\; \left(\frac{\partial \psi_i}{\partial \ddot{z}}\right)^T \;\middle|\; \left(\frac{\partial \psi_i}{\partial \mu}\right)^T \right]^T_j \tag{4.31}$$

The composite adjoint vector Λ^{ij}, as represented in Eq. 4.30, is a 12n x 1 vector. This vector can be written as a composite vector of four (3n×1) adjoint vectors λ_1^{ij} to λ_4^{ij}. Equation 4.31 can thus be expanded as

$$
\left[
\begin{array}{cccc}
\left(\dfrac{\partial\Phi}{\partial z}\right)^T &
\left[\dfrac{\partial}{\partial z}\left[\left(\dfrac{\partial\Phi}{\partial z}\right)\cdot z\right]\right]^T + \left[\dfrac{\partial}{\partial z}\left[\dfrac{\partial\Phi}{\partial\alpha}\right]\right]^T &
\left[\dfrac{\partial}{\partial z}\left[\left(\dfrac{\partial\Phi}{\partial z}\right):z\right]\right]^T + \left(\dfrac{\partial\Omega}{\partial z}\right)^T + \left[\dfrac{\partial}{\partial z}\left[\left(\dfrac{\partial\Phi}{\partial z}\right):z\right]\right]^T &
\left[\dfrac{\partial}{\partial z}\left(\dfrac{\partial\Phi}{\partial z}\right)^T u\right]^T \\[12pt]
0 &
\left(\dfrac{\partial\Phi}{\partial z}\right)^T &
\left[\dfrac{\partial}{\partial z}\left[\left(\dfrac{\partial\Phi}{\partial z}\right):z\right]\right]^T &
-\left(\dfrac{\partial G}{\partial z}\right)^T \\[12pt]
0 & 0 &
\left(\dfrac{\partial\Phi}{\partial z}\right)^T &
-\left(\dfrac{\partial G}{\partial \dot z}\right)^T \\[12pt]
0 & 0 & 0 &
-\left(\dfrac{\partial G}{\partial \ddot z}\right)^T
\end{array}
\right]_j
\left\{
\begin{array}{c}
\lambda_1^{ij} \\[8pt]
\lambda_2^{ij} \\[8pt]
\lambda_3^{ij} \\[8pt]
\lambda_4^{ij}
\end{array}
\right\}
=
\left\{
\begin{array}{c}
\left(\dfrac{\partial\psi_1}{\partial z}\right)^T \\[8pt]
\left(\dfrac{\partial\psi_1}{\partial \dot z}\right)^T \\[8pt]
\left(\dfrac{\partial\psi_1}{\partial \ddot z}\right)^T \\[8pt]
\left(\dfrac{\partial\psi_i}{\partial z^n}\right)^T
\end{array}
\right\}_j
\tag{4.32}
$$

Equation 4.32 is a system of 12n linear equations. Rather than solve this as a coupled system of 12n equations, the form of the coefficient matrix makes it possible to solve four separate linear systems of 3n equations each.

As can be seen from Eq. 4.32, there is no coupling between the adjoint vector λ_4^{ij} and any of the other adjoint vectors. Thus the last 3n equations can be written as

$$\left[\frac{\partial \Phi}{\partial z}\right]_j \lambda_4^{ij} = \left(\frac{\partial \psi_i}{\partial \mu}\right)_j^T \tag{4.33}$$

which has the same coefficient matrix as Eq. 2.19. As noted in Section 2.2.3, the solution of linear systems with this coefficient matrix is very efficient, since the LU factored form of the coefficient matrix has already been computed and stored.

Equations (6n + 1) to (9n) of Eq. 4.32 can then be written as

$$\left[\frac{\partial \Phi}{\partial z}\right]_j^T \lambda_3^{ij} - \left(\frac{\partial G}{\partial \ddot{z}}\right)_j^T \lambda_4^{ij} = \left[\frac{\partial \psi_i}{\partial \ddot{z}}\right]_j^T \tag{4.34}$$

Since λ_4^{ij} has already been determined as the solution of Eq. 4.33, Eq. 4.34 can be rewritten as

$$\left[\frac{\partial \Phi}{\partial z}\right]_j^T \lambda_3^{ij} = \left(\frac{\partial \psi_i}{\partial \ddot{z}}\right)_j^T + \left(\frac{\partial G}{\partial \ddot{z}}\right)_j^T \lambda_4^{ij} \tag{4.35}$$

The coefficient matrix in Eq. 4.35 is the transpose of the coefficient matrix of Eq. 2.19. The remarks made above about the solution efficiency of Eq. 4.33 are also valid for Eq. 4.35.

Continuing this process of backward solution, equations (3n+1) to (6n) of the linear system of Eq. 4.32 can now be written as

$$\left(\frac{\partial \Phi}{\partial z}\right)^T_j \lambda^{ij}_2 = \left(\frac{\partial \psi_i}{\partial \dot{z}}\right)^T_j - \left[\frac{\partial}{\partial \dot{z}}\left[\frac{\partial \Phi}{\partial z}\left[\left(\frac{\partial \Phi}{\partial z}\right)\dot{z}\right]\dot{z}\right]\right]^T_j + \lambda^{ij}_3 + \left(\frac{\partial G}{\partial \dot{z}}\right)^T_j \lambda^{ij}_4$$

$$(4.36)$$

where λ^{ij}_3 and λ^{ij}_4 are the solutions of Eqs. 4.35 and 4.33, respectively.

As in the case of Eq. 4.35, the coefficient matrix of Eq. 4.36 is the transpose of the coefficient matrix of Eq. 2.19, so the remarks made about the solution efficiency of Eq. 4.33 are also valid for Eq. 4.36.

The first 3n equations of the linear system in Eq. 4.32 can now be written as

$$\left[\frac{\partial \Phi}{\partial z}\right]^T_j \lambda^{ij}_1 = \left(\frac{\partial \psi_i}{\partial z}\right)^T_j - \left\{\left[\frac{\partial}{\partial z}\left[\left(\frac{\partial \Phi}{\partial z}\right)\dot{z}\right]\right]^T + \left[\frac{\partial}{\partial z}\left[\frac{\partial \Phi}{\partial \alpha}\dot{\alpha}\right]\right]^T\right\}_j \lambda^{ij}_2$$

$$- \left\{\left[\frac{\partial}{\partial z}\left[\left(\frac{\partial \Phi}{\partial z}\right)\ddot{z}\right]\right]^T + \left(\frac{\partial \Omega}{\partial z}\right)^T + \left[\frac{\partial}{\partial z}\left[\frac{\partial}{\partial z}\left[\left(\frac{\partial \Phi}{\partial z}\right)\dot{z}\right]\dot{z}\right]\right]^T\right\}_j \lambda^{ij}_3$$

$$- \left\{\left[\frac{\partial}{\partial z}\left[\left(\frac{\partial \Phi}{\partial z}\right)^T \mu\right]\right]^T - \left(\frac{\partial G}{\partial z}\right)^T\right\}_j \lambda^{ij}_4 \qquad (4.37)$$

where λ_2^{ij}, λ_3^{ij}, λ_4^{ij} are the solutions of Eqs. 4.36, 4.35 and 4.33, respectively. The coefficient matrix of Eq. 4.37 is the transpose of the coefficient matrix of Eq. 2.19, so the remarks made about the solution efficiency of equations with this coefficient matrix are also valid for Eq. 4.37.

Equations 4.33 and 4.35 to 4.37 are four adjoint equations associated with the four state equations. Now that the solution of the composite adjoint vector Λ^{ij^T} is known, Eq. 4.30 can be substituted into Eq. 4.29 to give

$$\delta\psi^{ij} = \left\{ \Lambda^{ij^T} B^j + \left(\frac{\partial\psi_i}{\partial b}\right)_j \right\} \delta b \qquad (4.38)$$

Equation 4.38 expresses the variation of a composite design constraint in terms of the variation in design only. Comparing Eqs. 4.21 and 4.38, it can be concluded that the quantity premultiplying δb in Eq. 4.38 is the design sensitivity vector of the ith constraint, at the jth grid point. Therefore,

$$\ell^{ij^T} = \Lambda^{ij^T} B^j + \left(\frac{\partial\psi_i}{\partial b}\right)_j$$

Substituting for B^j from Eq. 4.26, this can be explicitly written as

$$\ell^{ijT} = - \left\{ \lambda_1^{ijT} \left(\frac{\partial \Phi}{\partial b}\right)_j + \lambda_2^{ijT} \left[\frac{\partial}{\partial b} \left[\left(\frac{\partial \Phi}{\partial z}\right) \dot{z} \right] + \frac{\partial}{\partial b} \left[\frac{\partial \Phi}{\partial \alpha} \dot{\alpha} \right] \right]_j \right.$$

$$+ \quad \lambda_3^{ijT} \left[\frac{\partial}{\partial b} \left[\frac{\partial}{\partial b} \left[\left(\frac{\partial \Phi}{\partial z}\right) \dot{z} \right] \dot{z} \right] + \frac{\partial}{\partial b} \left[\left(\frac{\partial \Phi}{\partial z}\right) \ddot{z} \right] + \left(\frac{\partial \Omega}{\partial z}\right) \right]_j$$

$$\left. + \quad \lambda_4^{ijT} \left[\frac{\partial}{\partial b} \left[\left(\frac{\partial \Phi}{\partial z}\right)^T \mu \right] - \left(\frac{\partial G}{\partial b}\right) \right]_j - \left(\frac{\partial \psi_i}{\partial z}\right)_j \right\} \qquad (4.39)$$

Equation 4.39 gives the design sensitivity of a composite design constraint i at grid point j, in terms of derivatives of the position state equation and the adjoint variables.

4.4   Design Optimization Algorithm

4.4.1   Active Set Strategy

With the design sensitivity information computed in the previous section, one can proceed to implement the optimization algorithm of his choice.   The gradient projection algorithm with constraint error correction [20] has been used in the past in related applications [26, 27].   This algorithm is used here for design optimization.   Before implementing this algorithm for the present application, some observations can be made that will enhance efficiency of computation.

In connection with the composite design constraints of Eqs. 4.16 and 4.17, it can be observed that many design constraints can be put in

a simpler form than that indicated in these equations. Constraints that do not involve the state variables do not explicitly or implicitly depend on the input variables α. Such constraints are called 'nonparametric' constraints. Design constraints that involve the state variables are called 'parametric' constraints. It is necessary to make this distinction, since only the parametric constraints are required to be satisfied over the entire range of input variables α. For a given design, the nonparametric constraints need only be evaluated once. However, parametric constraints must be evaluated at all points on the interval of the input variables.

An active set strategy may be adopted to determine the reduced set $\tilde{\psi}$ of active constraints. Since equality constraints, parametric or nonparametric, are always active, they are always included in the active set $\tilde{\psi}$. Nonparametric inequality constraints that are ε-active are also included in the reduced set $\tilde{\psi}$. Parametric inequality constraints, due to their dependence on the input variable α, must be evaluated on all points on the grid of input variable α. Some computational efficiency can be realized from the fact that the gradient projection algorithm, as stated in the following section, allows only small changes in design leading to small changes in state. A design constraint with a large violation at a given design iteration may not be fully satisfied at the subsequent design iteration. This is so because the algorithm used for optimization here uses only first-order information about the design constraints. However, design constraints are generally nonlinear. The regions of the input variable grid in which a parametric inequality constraint is active are also not expected

to change rapidly from design iteration to iteration. It is thus possible to avoid evaluating, for a few design iterations, a parametric constraint in the region in which it is not E-active.

Design iterations in which the parametric constraint is evaluated at each point on the α grid are defined as 'sweep' iterations. Iterations in which the parametric constraint is evaluated only in the active region are called 'nonsweep' iterations. The interval between two 'sweep' iterations depends upon how rapidly the active regions are changing. For 'nonsweep' design iterations, it is not necessary to solve the state equations on the entire range of the input variable. Considerable computational saving can be realized by having a large number of 'nonsweep' iterations between successive 'sweep' iterations. Since new active regions can only be detected during 'sweep' iterations, having a large number of 'nonsweep' iterations separating two 'sweep' iterations could lead to new active regions going undetected for a number of design iterations.

Two alternative definitions could be used to define active regions on the grid of the input variable. The first definition, as shown in Fig. 4.1, involves determining the ε-active relative maxima of the constraint function on the α-grid. The active region is then defined to be the set of points at which the relative maxima occur and one grid point on either side of these grid points. The active region can thus be defined by the index set I_R,

$$I_R = \left\{ I_{R_L} \cup I_{R_M} \cup I_{R_R} \right\} \tag{4.40}$$
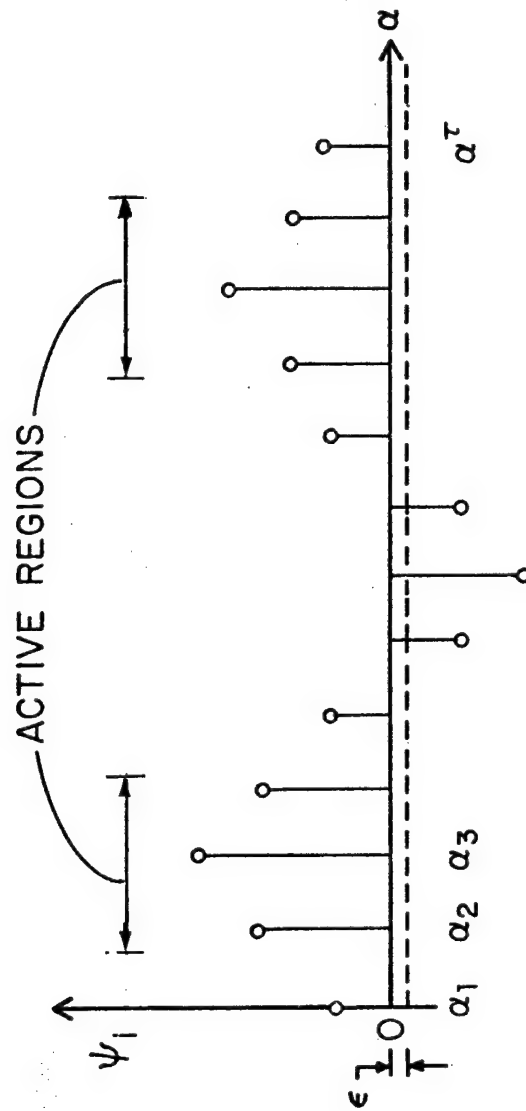
Figure 4.1 Definition of Active Regions on Basis of Relative
Maxima of Parametric Constraints

where

$$I_{R_M} = \{j-1, j, j+1 \mid \psi^{ij} \geqslant -\varepsilon, i = 1,\ldots,p, 2 \leqslant j \leqslant \tau-1;$$

is a relative maximum point $\}$

$$I_{R_L} = \{j, j+1 \mid \psi^{ij} \geqslant -\varepsilon, i = 1,\ldots,p, j = 1;$$

is a relative maximum point $\}$

$$I_{R_R} = \{j-1, j, \mid \psi^{ij} \geqslant -\varepsilon, i = 1,\ldots,p, j = \tau;$$

is a relative maximum point $\}$

The second definition of active region involves determining all the points on the α grid at which the constraint function is ε-active. This set is defined to be the ε-active region. Denoting this set as I_E,

$$I_E = \{j \mid \psi^{ij} \geqslant -\varepsilon, i = 1,\ldots,p, 1 \leqslant j \leqslant \tau\} \qquad (4.41)$$

The relative maximum strategy has been suggested for defining active regions for parametric constraints in Ref. [25]. When applied to constraints in mechanism optimization, this strategy many times causes rapid oscillation of the relative maximum point on the α-grid. A switch to the ε-active strategy overcomes this problem. As is evident from Figs. 4.1 and 4.2, there is a penalty to be paid for this switch, since the latter strategy requires a larger number of grid points to be included in the ε-active region.
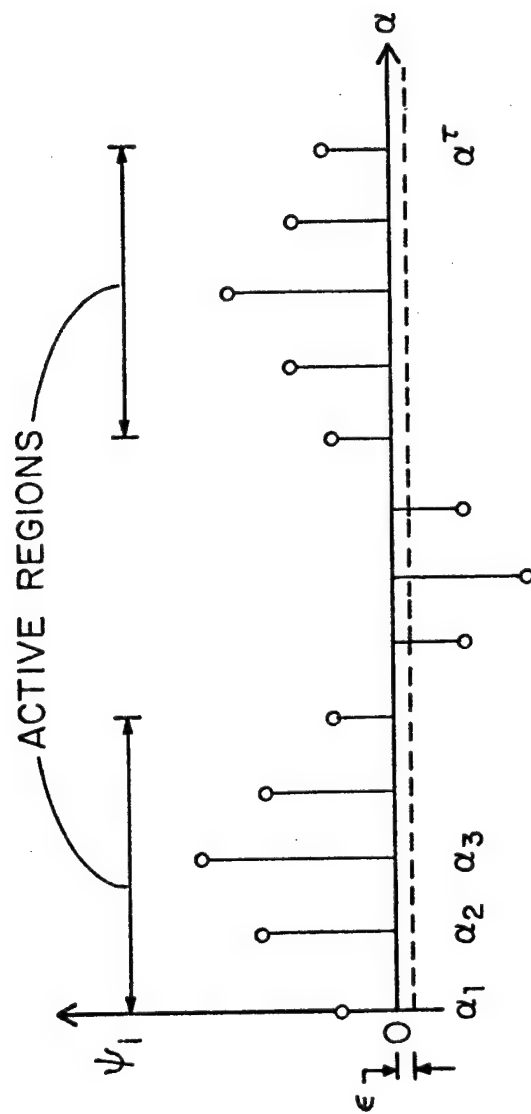
Figure 4.2 Definition of Active Regions on Basis of
Epsilon-Active Parametric Constraints

4.4.2 Gradient Projection Algorithm

The Gradient Projection Algorithm [20] for design optimization can now be stated in the following steps:,

Step 1: Estimate a design b^0, and impose a grid on the range of the input parameters.

Step 2: Solve the state equations of Eqs. 4.12 to 4.15 for state variables z^j, $\dot{z}^j$, $\ddot{z}^j$, μ^j, respectively, where $j = 1,\ldots,\tau$ if the current iteration is a 'sweep' design iteration or j I_R or I_E. Note, the first design iteration must be a sweep iteration.

Step 3: Determine the active region, depending on the strategy chosen, and form a reduced vector $\tilde{\psi}$ consisting of all ε-active non-parametric inequality, and all equality parametric and nonparametric constraints. For inequality parametric constraints, the constraints evaluated in the active regions are included in $\tilde{\psi}$.

Step 4: Compute adjoint variables λ_4^{ij}, λ_3^{ij}, λ_2^{ij}, and λ_1^{ij} from Eqs. 4.33, 4.35, 4.36 and 4.37, respectively, and construct design sensitivity vectors ℓ^{ij} of Eq. 4.39 for the constraint functions in $\tilde{\psi}$. Form the matrix $\tilde{\Lambda}=[\ell^{ij}]$, whose columns are the vectors ℓ^{ij} corresponding to constraint functions in $\tilde{\psi}$. Thus, $\delta\tilde{\psi} = \tilde{\Lambda}^T \delta b$

Step 5: Compute the vector $M_{\psi\psi_0}$ and matrix $M_{\psi\psi}$ from the following relations;

$$M_{\psi\psi_0} = \tilde{\Lambda}^T W^{-1} \ell^0 \qquad (4.42)$$

where ℓ^0 is defined in Eq. 4.18

$$M_{\psi\psi} = \tilde{\Lambda}^T W^{-1} \tilde{\Lambda} \qquad (4.43)$$

Step 6: In the first iteration, compute a parameter γ related to step size, as

$$\gamma = \frac{\ell^{0^T} W^{-1} \ell^0}{2\beta \, \psi_0(b^0)} \tag{4.44}$$

where β is the desired fractional reduction in the cost function. The usual range of β is 0.03 to 0.15. In succeeding iterations, the factor γ is adjusted to enhance convergence of the algorithm.

Step 7: Compute $\tilde{\mu}^1$ and $\tilde{\mu}^2$ from eqs. 4.45 and 4.46,

$$M_{\psi\psi} \tilde{\mu}^1 = -M_{\psi\psi_0} \tag{4.45}$$

$$M_{\psi\psi} \tilde{\mu}^2 = -\Delta\tilde{\psi} \tag{4.46}$$

where $\Delta\tilde{\psi} = C_\psi \tilde{\psi}$, C_ψ is the fraction correction of the constraint desired, usually in the range 0.30 to 1.0.

Step 8: Compute δb^1 and δb^2 from Eqs. 4.47 and 4.48 as

$$\delta b^1 = W^{-1} \left[\ell^0 + \Lambda \tilde{\mu}^1 \right] \tag{4.47}$$

$$\delta b^2 = -W^{-1} \Lambda \tilde{\mu}^2 \tag{4.48}$$

Step 9: Compute an update in design δb from Eq. 4.49

$$\delta b = -\frac{1}{2\gamma} \delta b^1 + \delta b^2 \tag{4.49}$$

Step 10: Update the estimate of the optimal design using Eq. 4.50

$$b^1 = b^0 + \delta b \tag{4.50}$$

Step 11:   If all constraints are satisfied to within the prescribed

tolerance and

$$||\delta b^1|| = \left[\sum_{i=1}^{S} W_i (\delta b^1_i)^2 \right]^{1/2} \leq \delta \qquad (4.51)$$

terminate the process.   Where δ is a specified convergence

tolerance.   If Eq. 4.51 is not satisfied, return to Step 2.

CHAPTER 5

NUMERICAL EXAMPLES

5.1 Example 1 – Kinematic Synthesis of a Path Generator

5.1.1 Problem Description

A segment of a straight line is required to be generated by a point P on the coupler of the four-bar mechanism shown in Fig. 5.1. In addition to having the lengths of various links as design variables (b_1 to b_3), the orientation of the base link, body 1, is a design variable (b_5). The orientation of the reference line with respect to the base link, about which the input variable α is measured, is also a design variable (b_4). The other two design variables (b_7 and b_8) are as indicated in Fig. 5.1. The length of the base link is kept fixed at 10 units. This problem is the same as Example 3 in Ref. 26.

5.1.2 Problem Formulation

The motion specification for this problem requires that the deviation of the y coordinate of coupler point P from zero in the global coordinate system be minimized. The position vector for point P, in terms of design and state variables, can be written as

$$\bar{R}_p = x_3 + \cos\theta_3\left(-\frac{b_2}{2} + b_7\cos b_8\right) - b_7\sin b_8\sin\theta_3 \quad \bar{I}$$

$$= y_3 + \sin\theta_3\left(-\frac{b_2}{2} + b_7\cos b_8\right) + b_7\cos\theta_3\sin b_8 \quad \bar{J} \quad (5.1)$$
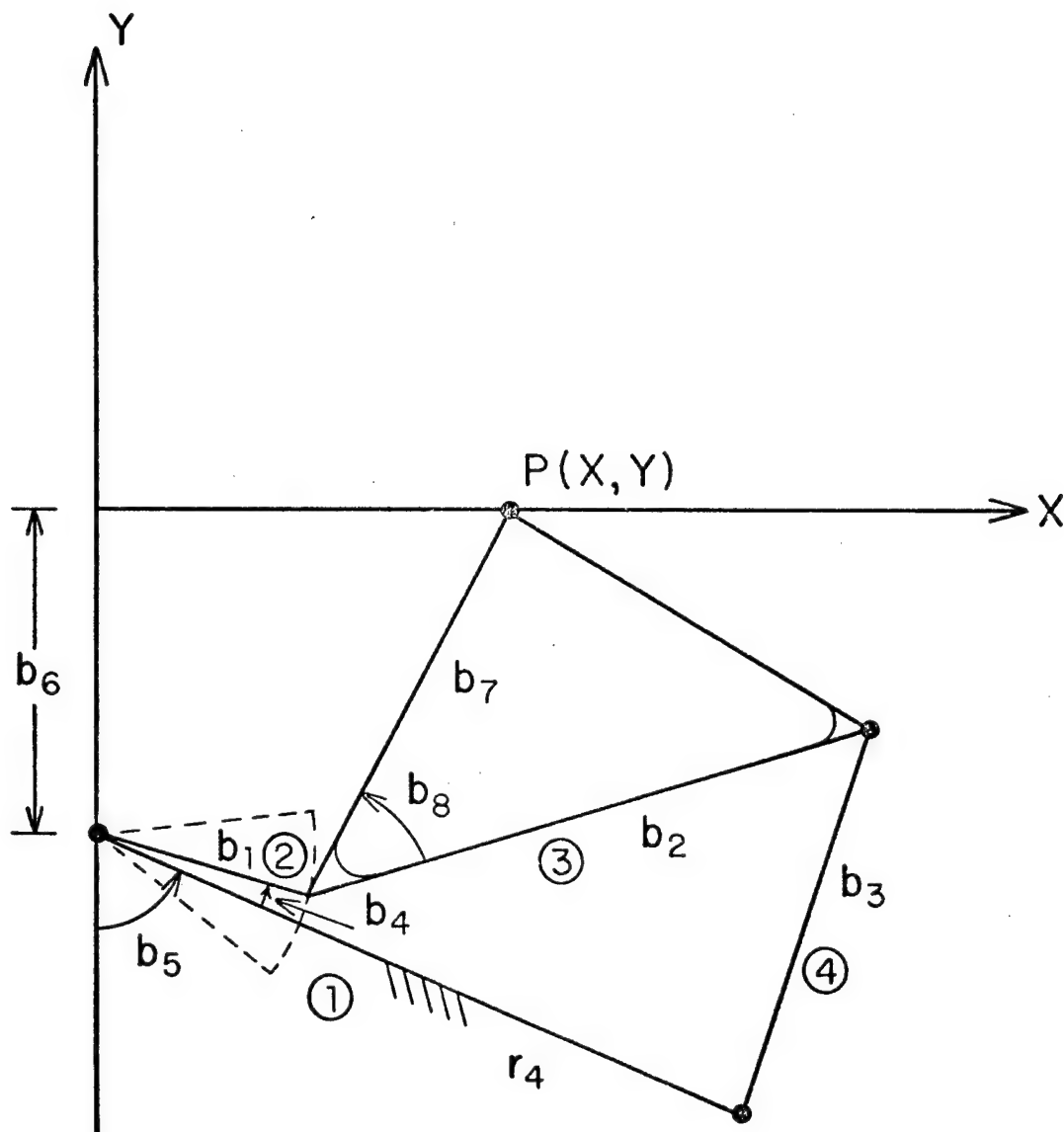
Figure 5.1   Four-Bar Path Generator Mechanism

Equation 5.1 can be symbolically expressed as

$$\bar{R}_p = (R_{p_x}) \bar{I} + (R_{p_y}) \bar{J} \qquad (5.2)$$

where R_{p_x} and R_{p_y} represent the x and y coordinates of point p in the global coordinate system.

An artificial design variable b_9 is introduced such that

$$\left| R_{p_y} \right| \leqslant b_9 \quad , \quad \alpha_{min} \leqslant \alpha \leqslant \alpha_{max}$$

where the range of α is given as $\alpha_{min} = -0.3491$ radians and $\alpha_{max} = 0.3491$ radians. This problem can now be formulated in the standard form given in Chapter 4; i.e., minimize

$$\text{Min } \psi_0 = b_9 \qquad (5.3)$$

subject to discretized design constraints

$$\psi_1^i \equiv \left| R_{p_y} \right|_i - b9 \leqslant 0 \ , \ i = 1, \ \ldots, \ \tau \qquad (5.4)$$

The constraint that the input link b_1 is a crank is imposed in the form [26]

$$\psi_2 \equiv \left| r_4 - b_2 \right| - b_3 + b_1 \leqslant 0 \qquad (5.5)$$

$$\psi_3 \equiv b_1 + b_3 - b_2 - r_4 \leqslant 0 \qquad (5.6)$$

Nonnegativity constraints on b_7 and b_8 are written in the form

$$\psi_4 \equiv -b_7 \leqslant 0 \qquad\qquad\qquad (5.7)$$

$$\psi_5 \equiv -b_8 \leqslant 0 \qquad\qquad\qquad (5.8)$$

The error bound constraint in Eq. 5.4 is imposed over a grid of $\tau = 19$ equally spaced points on the range of α. The driving kinematic constraint for this problem is given as

$$\phi_1^d \equiv \theta_2 - \{b_5 + b_4 + \alpha_1^i\} = 0 \quad , \qquad i = 1,\ldots,19$$

5.1.3 Numerical Results

5.1.3.1 Verification of Design Sensitivity Analysis

It is necessary to numerically verify that the technique developed in Chapter 4 has been correctly coded. The procedure used is briefly explained here.

The problem is set up through user supplied routines and input data. The code is allowed to run for 2 design iterations. On the basis of the design sensitivity vector calculated and the change in design δb obtained in the first iteration, changes in the constraint can be predicted. This predicted value can be compared with the actual change obtained when the constraint functions are evaluated in the second design iteration. If the design sensitivity analysis is valid, the predicted and actual changes in constraints should agree within a reasonable tolerance. This procedure is now used to verify the design sensitivity analysis for this problem. Consider grid point 19, where the parametric constraint of Eq. 5.4 is violated during a design iteration.

$$\ell^{1,19^T} = \begin{bmatrix} -0.67893, & -.04693, & 0.06083, & 2.30624, & 2.85158, & -1.0, \\ & 0.99853, & 0.34923, & -1.0 \end{bmatrix}$$

The change in design at this iteration is $\delta b^T = \begin{bmatrix} 0.01663, & 0.00115, \end{bmatrix}$ $-0.00149, \ -0.05650, \ -0.06985, \ 0.02450, \ -0.02446, \ -0.00853, \ -0.2096 \big].$ The predicted change in the constraint is thus given as

$$\Delta\psi_p^{1,19} = \ell^{1,19^T} \delta b = -0.1832$$

The actual change in the constraint function is evaluated as

$$\Delta\psi_A^{1,19} = -0.1709$$

The difference between the predicted and actual change is 6.7%. The design sensitivity analysis is thus considered to be valid.

5.1.3.2 Optimization Results

The results obtained from the optimization procedure are as presented in Table 5.1. None of the nonparametric constraints was active at the optimum. As given in Table 5.1, there are 5 critical points on the grid of the input parameter at the optimum design, where the error in function generation is a relative maximum. The maximum error obtained in Ref. 26 for this problem was about 0.0019, which is greater than that obtained by the present technique.

Table 5.1   Results for Example 1

	b_1	b_2	b_3	b_4	b_5	b_6	b_7	b_8	
Initial Design	3.5	9.0	10.0	0.0	-1.0	-2.5	6.5	1.0	1.36
Final Design (38th iter)	3.2463	9.3608	6.8637	-.2455	-0.7762	-2.7825	7.3475	0.6532	0.001175

Critical grid points at Final Design:

-0.3491	-0.2327	0.0	0.2327	0.3491

Error at critical grid points:

0.001092	0.001175	0.001175	0.0011705	0.001096

At the final design $||\delta b^1|| = 5 \times 10^{-3}$

Computing time on IBM 370/168 approximately 0.39 secs/iteration

5.2 Example 2: Kinematic Synthesis of a
Rigid Body Guidance Mechanism

5.2.1 Problem Description

The mechanism shown in Fig. 5.2 is to guide the book-carriage of a library book-stacking vehicle [28]. It is required that point P describe a path given in Table 5.2. In addition it is required that body 8, the carrier, assume angular orientation at specific input grid points, given in Table 5.2. The mechanism is driven by the rotating crank, which is body 4.

Design variables b_1, b_2, and b_3 radially locate the 3 joints of the ternary base link. The angular orientation of these radial lines is specified by the three angles $\beta_1 = 73.5°$, $\beta_2 = 61.5°$, and $\beta_3 = 71.5°$. Design variables b_4 to b_9 are the lengths of links 4 to 9, respectively. The length of link 10 is taken as 10 units. Other angles specified in Fig. 5.2 are given as $\beta_4 = -50.0°$, $\beta_5 = -63.0°$, and $\beta_6 = -103.0871°$.

5.2.2 Problem Formulation

The global x and y coordinates of the coupler point P can be written in terms of design and state variables as

$$\bar{R}_p = \{x_8 + \cos\theta_8(\frac{b_8}{2} - A\cos\beta_4) - A\sin\theta_8\sin\beta_4\}\,\bar{I}$$

$$+ \{y_8 + \sin\theta_8(\frac{b_8}{2} - A\cos\beta_4) + A\cos\theta_8\sin\beta_4\}\,\bar{J} \qquad (5.9)$$

Equation 5.9 can be symbolically written as

$$\bar{R}_p = (R_{p_x})\,\bar{I} + (R_{p_y})\,\bar{J} \qquad (5.10)$$
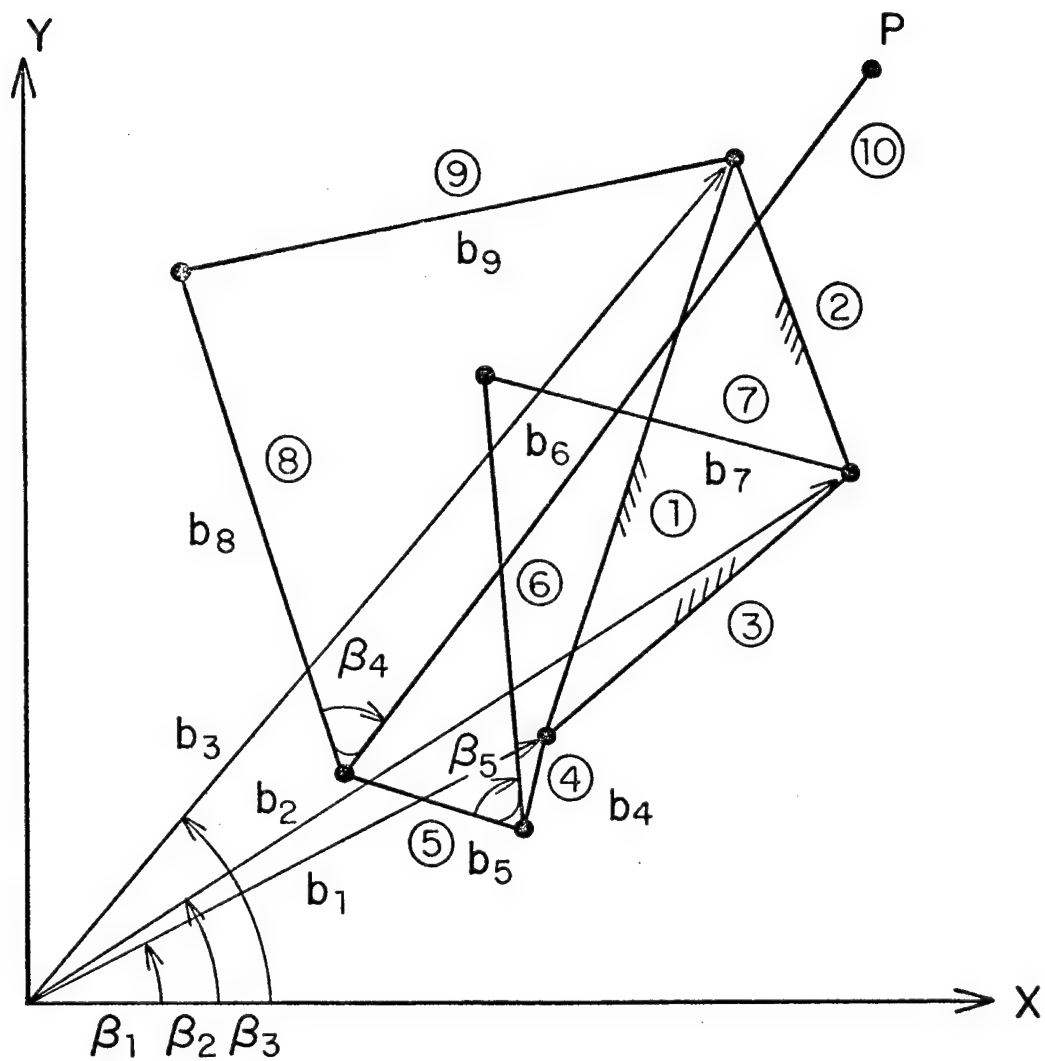
Figure 5.2 Rigid-Body Guidance Problem

Table 5.2 Output Specifications for Example 2

Grid pt	θ_4 (deg)	$(P_x)_d$ cms	$(P_y)_d$ cms	$(\theta_8)_d$ (deg)
1	−62.5	11.943	6.458	103.0871
2	−40.5	12.712	6.288	107.9571
3	23.0	13.214	6.075	111.2971
4	0.0	14.553	5.774	114.2471
5	31.0	15.824	5.716	113.5876
6	50.5	16.396	5.71	110.3871
7	78.5	16.388	6.465	103.0871

where R_{P_x} and R_{P_y} represent the x and y components of the position vector of point P.

An artificial design variable b_{10} is now introduced to impose the following constraints:

$$\left| (R_{P_x}) - (p_x)_d \right|_j \leq c_1 b_{10} \quad , \; j = 1, \ldots, 7$$

$$\left| (R_{P_y}) - (p_y)_d \right|_j \leq c_2 b_{10} \quad , \; j = 1, \ldots, 7$$

$$\left| (\theta_8)_g - (\theta_8)_d \right|_j \leq c_3 b_{10} \quad , \; j = 1, \ldots, 7$$

where $(p_x)_d$ and $(p_y)_d$ are the desired x and y coordinates of point p, $(\theta_8)_d$ is the desired orientation of link 8 and $(\theta_8)_g$ is the generated orientation of link 8.

In standard form, this problem is formulated as; minimize

$$\psi_0 \equiv b_{10} \tag{5.11}$$

subject to discretized design constraints

$$\psi_1^j \equiv \left| (R_{P_x}) - (p_x)_d \right|_j - c_1 b_{10} \leq 0 , \quad j = 1, \ldots, 7 \tag{5.12}$$

$$\psi_2^j \equiv \left| (R_{P_y}) - (p_y)_d \right|_j - c_2 b_{10} \leq 0 , \quad j = 1, \ldots, 7 \tag{5.13}$$

$$\psi_3^j \equiv \left| (\theta_8)_g - (\theta_8)_d \right|_j - c_3 b_{10} \leq 0 , \quad j = 1, \ldots, 7 \tag{5.14}$$

The driving kinematic constraint for this problem is given as:

$$\phi_1^d \equiv \theta_1^d - \alpha_1^i = 0 , \quad i = 1, \ldots, 7$$

5.2.3 Numerical Results

5.2.3.1 Verification of Design Sensitivity Analysis

The procedure outlined in Section 5.1.3.1 is used here to verify the design sensitivity analysis. The design sensitivity vectors at a certain iteration for the three error constraints were obtained as

$$\ell^{1,1^T} = [-0.44247, -0.05346, 0.77940, 0.44687, 0.01196, -0.06584,$$
$$0.16044, -0.18837, -1.19525, -1.0]$$

$$\ell^{2,4^T} = [-1.42060, 0.03326, 0.32397, -0.13204, 0.48655,$$
$$-0.46958, 0.60349, 0.14956, -0.65320, -1.0]$$

$$\ell^{3,6^T} = [0.24504, -0.15474, -0.08915, 0.51890, -0.82560, 0.20605,$$
$$-0.23002, -0.49248, 0.88695, -1.0]$$

The change in design obtained at this iteration was

$$\delta b^T = [-0.00368, 0.02838, -.001735, 0.002504, 0.01337, 0.02730,$$
$$0.00148, -.00806, 0.003155, -0.002811]$$

The predicted changes in the constraints can thus be computed as,

$$\Delta\psi_p^{1,1} = \ell^{1,1^T} \delta b = -0.00096$$

$$\Delta\psi_p^{2,4} = \ell^{2,4^T} \delta b = -0.00060$$

$$\Delta\psi_p^{3,6} = \ell^{3,6^T} \delta T = -0.000014$$

The actual changes in these constraint functions were

$$\Delta\psi_A^{1,1} = (0.003869 - 0.004834) = -0.000965$$

$$\Delta\psi_A^{2,4} = (0.0023898 - 0.002992) = -0.000604$$

$$\Delta\psi_A^{3,6} = (0.00006938 - 0.00008909) = -0.0000197$$

Comparison of the actual and predicted changes in the constraints shows that for the first two constraints there is a good agreement. However, for the third constraint the agreement is not as good. This can be attributed to numerical error in differencing very small numbers

5.2.3.2 Optimization Results

The results from the optimization procedure are presented in Table 5.3. The first parametric constraint was active at 3 critical points, the second at 2 critical points, and the third at only one critical point. The maximum error obtained using the present technique is 20% higher than that reported in Ref. 28.

5.3 Example 3 -- Two degree of Freedom Function Generator

5.3.1 Problem Description

The relationship $u = (1 + v)\log_{10}(1 + w)$ is to be mechanized in the region $0 \leqslant v \leqslant 1$, and $0 \leqslant w \leqslant 1$. This problem is similar to the numerical example given in Ref. 6. The mechanism to be used for function generation is a seven-link mechanism shown in Fig. 5.3. The inputs v and w are the displacements of bodies 5 and 6, respectively. These displacements are measured from reference positions, measured along the global axis, which are taken as design variables b_1 and b_2. The output u of the mechanism, is the displacement of body 2 relative to the origin of the global coordinate system. This displacement is measured along the line of translation that makes an angle $\gamma = 27.881°$ with respect to the global x-axis. the lengths of links 3, 4, 6 and 7 are design variables b_4 to b_7. The angle between links 4 and 6 is

Table 5.3   Results for Example 2

	b_1	b_2	b_3	b_4	b_5	b_6	b_7	b_8	b_9	Max. Error
Initial Design	5.0	10.0	12.0	1.5	1.4	6.0	4.2	6.5	5.5	1.70
Final Design (45th iter)	5.3658	10.1524	13.3494	1.7987	1.9615	6.2622	3.979	6.6819	5.6762	0.027

	b_6	b_7	b_9
Critical grid points for Eq. 5.12	$-62.5°$	$-50.5°$	78.5
Error at critical grid points in Eq. 5.12	0.026	0.027	0.025
Critical point for Eq. 5.13	$-23.0°$	$31.0°$	
Error at critical points in Eq. 5.13	0.027	0.025	
Critical points for Eq. 5.14	$50.5°$		
Error at critical points in Eq. 5.14	0.025		

At the final design $||\delta b^1|| = 1.3 \times 10^{-2}$

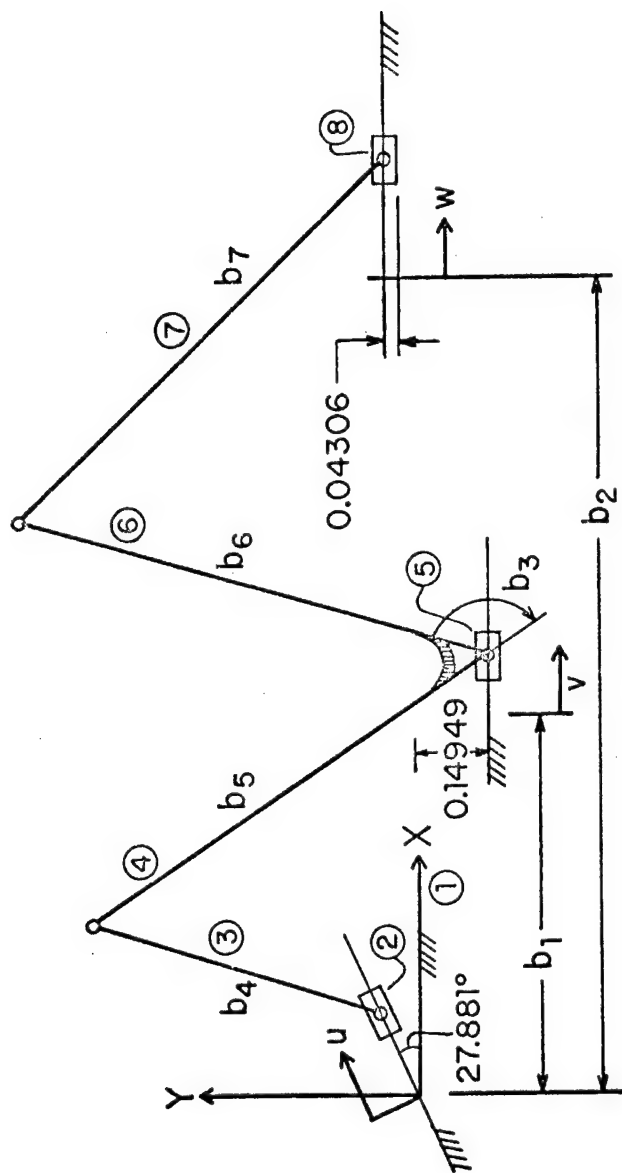Computing time on IBM 370/168 approximately 3.5 Secs/Iteration

Figure 5.3 Two Degree-of-Freedom Function Generator

design variable b_3. The other parameters related to this problem are as indicated in the Fig. 5.3.

5.3.2 Problem Formulation

The displacement of the output slider, body 2, along the line of translation can be written in terms of the generalized coordinates of body 2, as

$$U = \frac{x_2}{\cos \beta_1} \tag{5.15}$$

where $\beta_1 = 27.881°$.

An artificial design variable b_8 is introduced such that

$$\left| u_g - u_d \right|_{j,k} \leqslant b_8 \qquad \begin{array}{l} j = 1, \ldots, 4 \\ k = 1, \ldots, 4 \end{array}$$

where $(u_g)_{j,k}$ represents the generated value of u, for specific values of the input parameters α_1^j and α_2^k, and $(u_d)_{j,k}$ is the desired value of u, for the same values of the input parameters α_1^j and α_2^k. The function to be generated in this example,

$$(u_d)_{j,K} = (1 + \alpha_1^j) \log_{10}(1 + \alpha_2^k)$$

This problem can be formulated in standard form as; minimize

$$\psi_0 \equiv b_8 \tag{5.16}$$

Subject to discretized design constraints

$$\psi^{1, j, k} \equiv \left| (U_g)_{j,k} - (1 + \alpha_1^j) \log_{10}(1 + \alpha_2^k) \right| - b_8 \leqslant 0,$$

$$j,k = 1, \ldots, 4 \tag{5.17}$$

The error bound constraint is imposed on a grid of four equally spaced points, Fig. 5.4, on each of the input variables α_1 and α_2. Thus a total of 16 grid points are obtained. No other design constraints are imposed in this problem. The driving kinematic constraints for this problem are given as

$$\phi_1^d \equiv x_5 - (b_1 + \alpha_1^j) = 0 \quad , \qquad j = 1,\ldots,4$$

$$\phi_2^d \equiv x_8 - (b_2 + \alpha_2^k) = 0 \quad , \qquad k = 1,\ldots,4$$

5.3.3 Numerical Results

5.3.3.1 Verification of Design Sensitivity Analysis

The design sensitivity of the upper bound constraint, Eq. 5.17, at iteration no. 11 and grid point $j = 1$, $k = 4$ was obtained as

$$\ell^{1,1,4^T} = \big[0.15546, \ 0.23616, \ -0.57531, \ -1.45199, \ 1.29105, \ 0.06958,$$
$$-0.32795, \ -1.0\big]$$

The change δb in design was

$$\delta b^T = \big[-0.01027, \ 0.00197, \ 0.01753, \ 0.00938, \ 0.01017, \ 0.01178,$$
$$-0.00640, \ -0.00070\big]$$

The predicted change in constraint is thus computed as

$$\Delta \psi_p^{1,1,4} = \ell^{1,1,4^T} \delta b = -0.00805$$

The actual change in constraint was obtained as

$$\Delta \psi_A^{1,1,4} = 0.07259 - 0.08055 = -0.00796$$
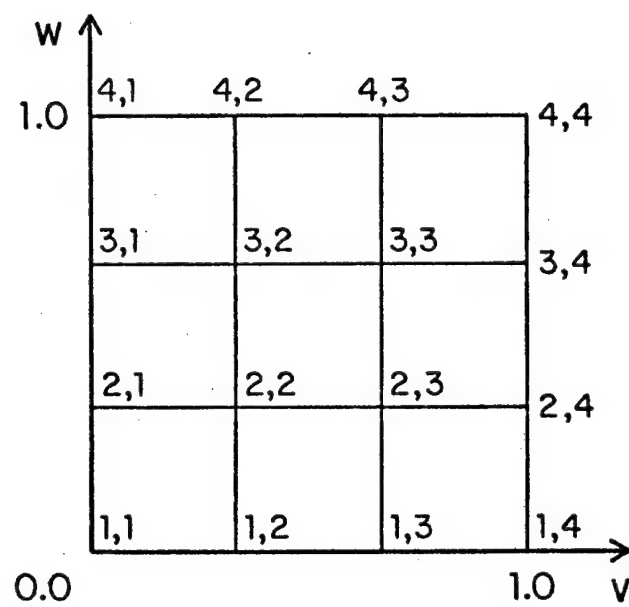
Figure 5.4   Grid Spacing for Problem 3

The difference between the actual and predicted change in the constraint is 1.0%, which verifies that the design sensitivity analysis for upper bound constraint of Eq. 5.17 is valid.

5.3.3.2 Optimization Results

The results of the optimization procedure for this problem are as presented in Table 5.4. The maximum error in function generation obtained from the present procedure is about 25% higher than that obtained in Ref. 6. This can be attributed to 2 differences in the formulation. First, the design variables used in the present problem and Ref. 6 are not the same. Second, the grid points in the present formulation and Ref. 6 are not identical. Location of grid points is known to have a very significant effect on the error in function generation [14].

5.4 Example 4 – Stress Constrained Design of a Four-Bar Mechanism

5.4.1 Problem Description

The four-bar mechanism shown in Fig. 5.5 has its input crank rotating at a constant angular velocity of 300 rpm. This mechanism is to be designed for minimum mass, requiring that bending stresses in mobile links 2, 3, and 4 do not exceed an allowable stress. The design variables in the mechanism are the circular cross-sectional areas of the three mobile links. The link lengths are kept fixed at the values specified in Table 5.5. The mass density and allowable stress in the links are as given in Table 5.5. Specifications for this problem are the same as those of example 1 in Ref. 30 and example 1 in Ref. 29.

Table 5.4 Results for Example 3

	b_1	b_2	b_3	b_4	b_5	b_6	b_7	Max Error
Initial Design	0.750	2.4	-2.792	0.7	0.8	1.5	2.4	0.05
Final Design (30th iter)	0.538	2.45	-2.46	0.942	1.1152	1.687	2.159	0.006

At the final design $||\delta b^1|| = 1 \times 10^{-4}$

Computing time on IBM 370/168 approximately 1.0 Secs/Iteration
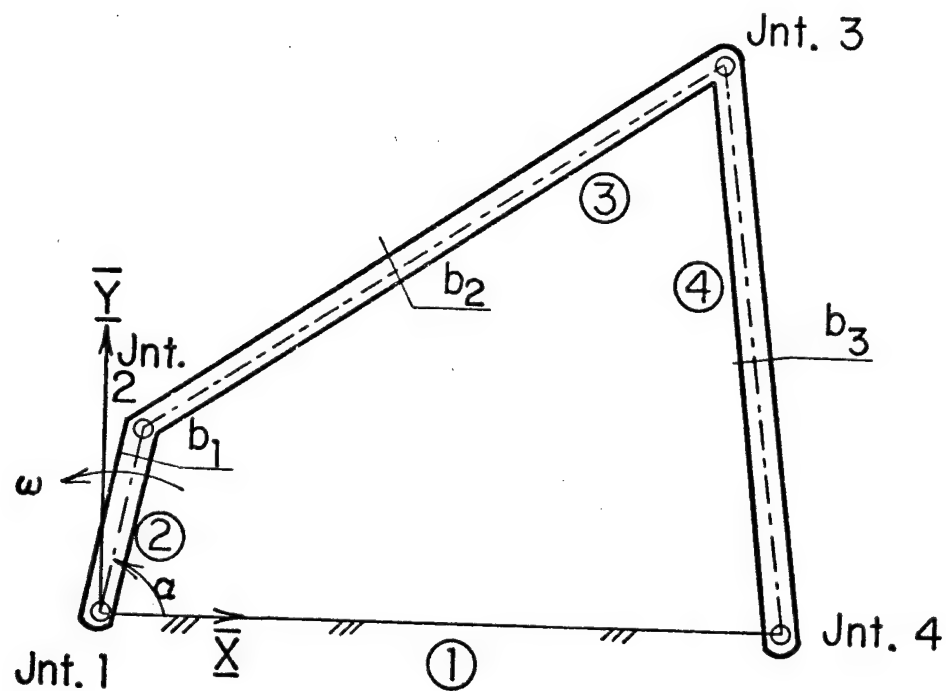
Figure 5.5 Minimum Weight Design of Four-Bar Mechanism

Table 5.5   Data for Example 4

	LINK			
	1	2	3	4
Length (m)	0.9144	0.3048	0.9144	0.762
mass density (kg/m^3)	--	2757.25	2757.24	2757.24
Modulus of Elasticity (Pa)	--	6.8948×10^{10}	6.8948×10^{10}	6.8948×10^{10}
Stress upper bound (Pa)	--	2.7579×10^7	2.7579×10^7	2.7579×10^7

5.4.2 Problem Formulation

As shown in Chapter 3, the Lagrange multipliers obtained as a solution of the force equation are directly related to reaction forces in the joints. As shown in Fig. 5.6, reactions at the ends of a link could thus be represented by the appropriate Lagrange multipliers. However, to compute bending moments, the end reactions are required to be expressed in a local coordinate system. As shown in Fig. 5.6, the μ_k, μ_{k+1} system of forces at a joint must be transformed to the P_k, P_{k+1} system.

The external load on the beam depends upon the normal acceleration. To compute the distribution of normal acceleration along the length of the link, a cross section of the link at distance ν along the x axis is considered. The position vector for point c can be written as

$$\bar{R}_{c_i} = x_i \ \bar{I} + y_i \ \bar{J} + \nu(\cos \theta_i \ \bar{I} + \sin \theta \ \bar{J}) \qquad (5.18)$$

where x_i, y_i and θ_i are the three generalized coordinates locating the body in the plane and $\bar{I}$ and $\bar{J}$ are unit vectors in the global $\bar{X}$ and $\bar{Y}$ directions.

The absolute acceleration of point c can thus be written as

$$\ddot{\bar{R}}_{c_i} = (\ddot{x}_i - \nu \cos \theta_i \ \dot{\theta}_i^2 - \nu \sin \theta_i \ \ddot{\theta}_i) \ \bar{I} +$$
$$(\ddot{y}_i - \nu \sin \theta_i \ \dot{\theta}_i^2 + \nu \cos \theta_i \ \ddot{\theta}_i) \ \bar{J}$$

Transforming the global unit vectors to the local system, acceleration normal to the length of the link can be written as
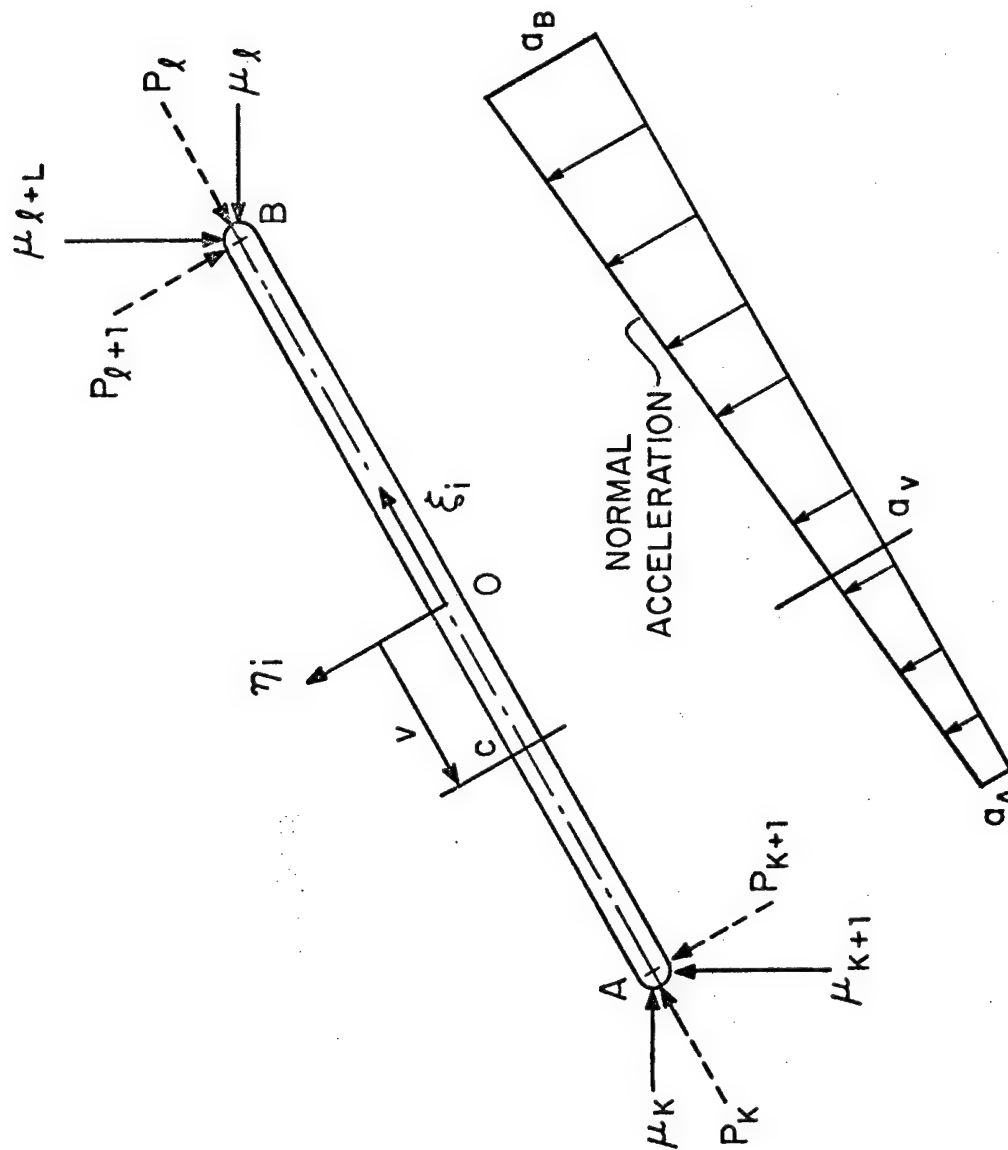
Figure 5.6 Loading System in Problem 4

$$a_{y_i} = (- \ddot{x}_i \sin \theta_i + \ddot{y}_i \cos \theta_i) + \nu \, \ddot{\theta}_i \qquad (5.19)$$

where $\ddot{x}_i$, $\ddot{y}_i$ and $\ddot{\theta}_i$ are the generalized accelerations of body i. From Eq. 5.19, it can be seen that the normal acceleration varies linearly along the length of the link.

The distributed loading on the beam can thus be written as

$$f_i = -m_{\ell_i} \{(-\ddot{x}_i \sin \theta_i + \ddot{y}_i \cos \theta_i) + \nu \, \ddot{\theta}_i\} \qquad (5.20)$$

where m_{ℓ_i} is mass per unit length of link i.

Equation 5.20 can be written as

$$f_i = -m_{\ell_i} \, a_{\ell_i} + \nu \, \ddot{\theta}_i \qquad (5.21)$$

where $a_{\ell_i} = -\ddot{x}_i \sin \theta_i + \ddot{y}_i \cos \theta_i$.

Since elementary beam theory is used to compute bending stresses, it is necessary to first determine the point of maximum bending moment. This is the point at which the shear force changes sign. The shear force at any point D, at a distance X_0 from 0, can be written as

$$F_s = P_{k+1} + -m_{\ell_i} \int_{-\ell i/2}^{X_0} (a_{\ell_i} + \nu \, \ddot{\theta}_i) \, d\nu$$

$$= P_{k+1} - m_{\ell_i} \left\{ a_{\ell_i} \left(x_0 + \frac{\ell_i}{2} \right) + \frac{\ddot{\theta}_i}{2} \left(x_0^2 - \frac{\ell_i^2}{4} \right) \right\} \qquad (5.22)$$

At the point of zero shear force, the right-hand side of Eq. 5.22 will be zero, giving rise to the condition

$$\frac{\ddot{\theta}_i}{2} X_0^2 + a_{\ell_i} X_0 + \left(\frac{a_{\ell_i}\ell_i}{2} - \frac{\ell_i^2 \ddot{\theta}_i}{8} - \frac{P_{k+1}}{m_{\ell_i}}\right) = 0 \qquad (5.23)$$

Solving for X_0 from Eq. 5.23,

$$X_0 = \frac{-a_{\ell_i} \pm \sqrt{a_{\ell_i}^2 - 2\ddot{\theta}_i\,\frac{a_{\ell_i}\ell_i}{2} - \frac{\ell_i^2 \ddot{\theta}_i}{8} - \frac{P_{k+1}}{m_{\ell_i}}}}{\ddot{\theta}_i} \qquad (5.24)$$

The maximum bending moment can thus be written as

$$M_{0_i} = P_{k+1}\left(\frac{\ell_i}{2} + X_0\right) + m_\ell \int_{-\ell/2}^{X_0} \left(a_{\ell_i} + v\,\ddot{\theta}_i\right)\left(\eta - X_0\right) dv \qquad (5.25)$$

Integration of Eq. 5.25 gives

$$M_{0_i} = P_{k+1}\left(\frac{\ell_i}{2} + X_0\right) + m_\ell \left\{ a_{\ell_i}\left[-\frac{X_0^2}{2} - \left(\frac{\ell_i^2}{8} + \frac{\ell_i X_0}{2}\right)\right] \right.$$
$$\left. + \ddot{\theta}_i \left[-\frac{X_0^3}{6} + \frac{\ell_i^3}{24} + \frac{X_0 \ell_i^2}{8}\right] \right\} \qquad (5.26)$$

where X_0 is given by Eq. 5.24.

Equation 5.26 is valid only for links 3 and 4. The crank, link 2, is rotating at constant angular velocity and has no normal acceleration. The maximum moment on this link is the torque required to drive the mechanism. It occurs at $\eta = -\frac{\ell_1}{2}$ and is given as

$$M_{0_2} = \mu_{12} \qquad (5.27)$$

Since the links are of circular cross section, the area moments of inertia can be written in terms of the design variables as

$$I_i = \frac{b_{i-1}^2}{4\pi} \tag{5.28}$$

where $2 \leqslant i \leqslant 4$ is the link number. The distance of the extreme fiber from the neutral axis is given as

$$y_i = \sqrt{\frac{b_{i-1}}{\pi}}$$

The absolute values of the maximum bending stresses, from elementary beam theory [31], can now be written as

$$(\sigma_b)_i = \frac{4}{b_{i-1}^{3/2}} \pi \left| M_0 \right| , \quad 2 \leqslant i \leqslant 4 \tag{5.29}$$

where M_0 is given by Eq. 5.27 for $i = 2$ and by Eq. 5.26 for $i = 3$ and 4

The optimization problem can be written in standard form as; minimize

$$\psi_0 \equiv \rho_2 \, \ell_2 \, b_1 + \rho_3 \, \ell_3 \, b_2 + \rho_4 \, \ell_4 \, b_3 \tag{5.30}$$

where ρ_i is mass density of link i, subject to discretized design constraints

$$\psi_k^j \equiv \frac{(\sigma_b^j)_{k+1}}{\sigma_a} - 1 \leqslant 0 , \quad j = 1, \ldots, \tau \tag{5.31}$$
$$1 \leqslant K \leqslant 3$$

where σ_a is allowable stress and τ is the total number of grid points. For this problem 19 grid points were considered. The driving constraint for this problem is given as

$$\phi_1^d \equiv \theta_2 - \alpha_1^j = 0 , \qquad j = 1, \ldots, 19$$

5.4.3   Numerical Results

5.4.3.1   Verification of Design Sensitivity Analysis

The design sensitivities of the stress constraints at a certain
iteration were obtained as

$$\ell^{1,17^T} = [-1801.18, \ 1928.83, \ 853.239]^T$$

$$\ell^{2,15^T} = [\quad 0.0 \ , -3481.67, \quad 0.0 \quad]^T$$

$$\ell^{3,15^T} = [\quad 0.0 \ , \quad 0.0 \ , +2051.6 \ ]^T$$

The change in design at this iteration was

$$\delta b^T = [2.022 \times 10^{-5}, \ 1.76 \times 10^{-5}, \ -8.626 \times 10^{-6}]$$

The predicted changes in the constraints can thus be computed as

$$\Delta \psi_P^{1,17} = \ell^{1,17^T} \ \delta b = -0.00983$$

$$\Delta \psi_P^{2,15} = \ell^{2,15^T} \ \delta b = -0.0613$$

$$\Delta \psi_P^{3,15} = \ell^{3,15^T} \ \delta b = -0.01739$$

The actual changes in the constraint function were obtined as

$$\Delta \psi_A^{1,17} = -0.0097$$

$$\Delta \psi_A^{2,15} = -0.06002$$

$$\Delta \psi_A^{3,15} = -0.0169$$

Comparison of the actual and predicted changes shows that the two
sets of data agree to within 2.5%. The design sensitivity analysis can
thus be considered valid.

5.4.3.2 Optimization Results

Results of the optimization procedure are presented in Table 5.6. Results obtained in Refs. 29 and 30 for this problem are also given. As can be seen, there is a substantial difference between the designs obtained. This difference is attributed to the fact that Refs. 29 and 30 use different methods for stress analysis than used in the present formulation. The constraint functions are, therefore, not identical.

5.5   Example 5 – Dynamic Balancing of a Four-Bar Mechanism

5.5.1   Problem Description

It is desirable to make the shaking forces of a mechanism vanish by balancing the mechanism. However, doing so introduces additional difficulties. For example, the RMS bearing forces could increase by as much as 100 percent [4]. In the present example, the four-bar mechanism shown in Fig. 5.7 is considered. A trade-off is resorted to, in which the RMS shaking forces are minimized, while limiting increase in the ground-bearing forces. Minimization of RMS shaking force is accomplished by modifying the inertial properties of the output, link by adding a circular counterweight to it, as shown in Fig. 5.8. The mass and location of this counterweight are design variables.

Data for the mechanism considered in this problem are given in Table 5.7. This problem is the same as the single counterweight optimization example given in Ref. 4.

Table 5.6   Results for Example 4

	Design Variables			Mass (kg)
	$b_1(m^2)$	$b_2(m^2)$	$b_3(m^2)$	
Starting Design	$1 \times 10{-}1$	$1 \times 10{-}1$	$1 \times 10{-}1$	546.26
Optimal Design 30th iter	$1.03 \times 10{-}3$	$0.621 \times 10{-}3$	$0.1169 \times 10{-}3$	2.686
Results from Reference 29	$0.401 \times 10{-}3$	$0.385 \times 10{-}3$	$0.385 \times 10{-}3$	2.134
Results from Reference 30	$0.953 \times 10{-}3$	$0.488 \times 10{-}3$	$0.309 \times 10{-}3$	2.703

At the final design $||\delta b^1|| = 2.5 \times 10^{-6}$

Approximate CPU time (IBM 370/168) = 1.25 Sec/Iteration

94
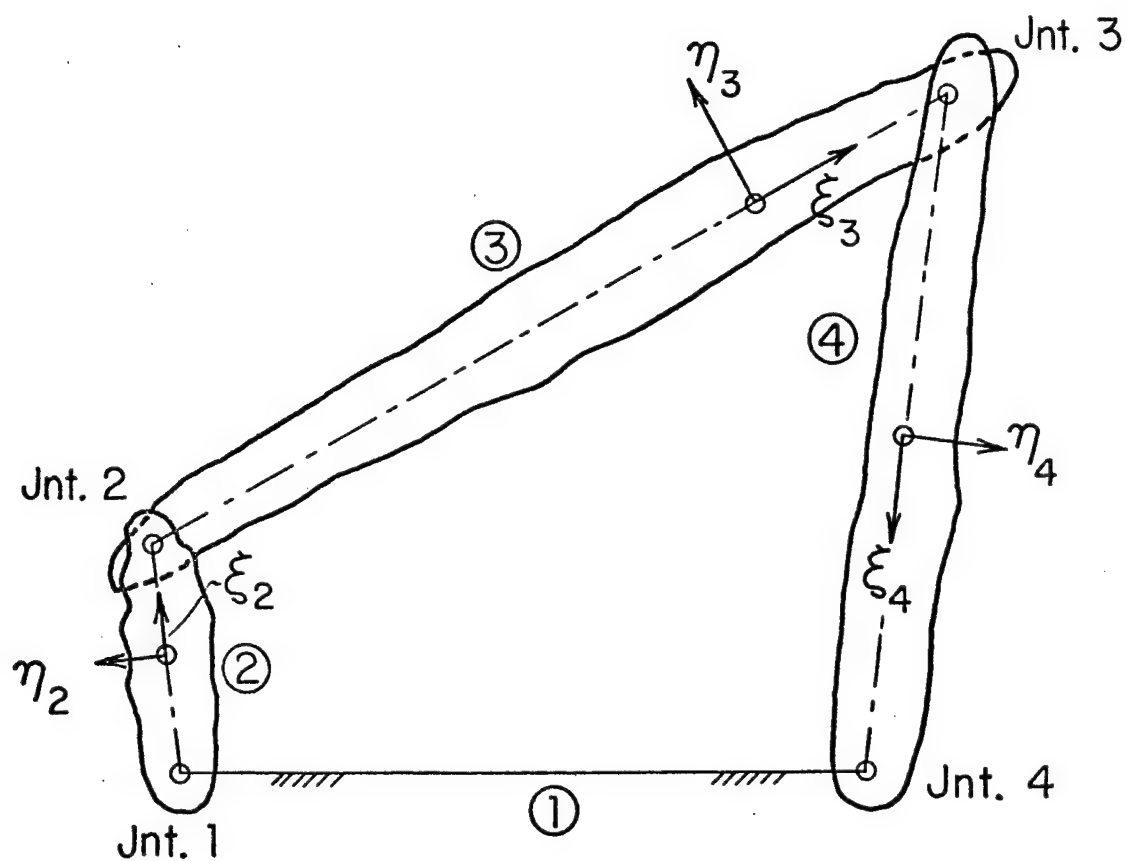

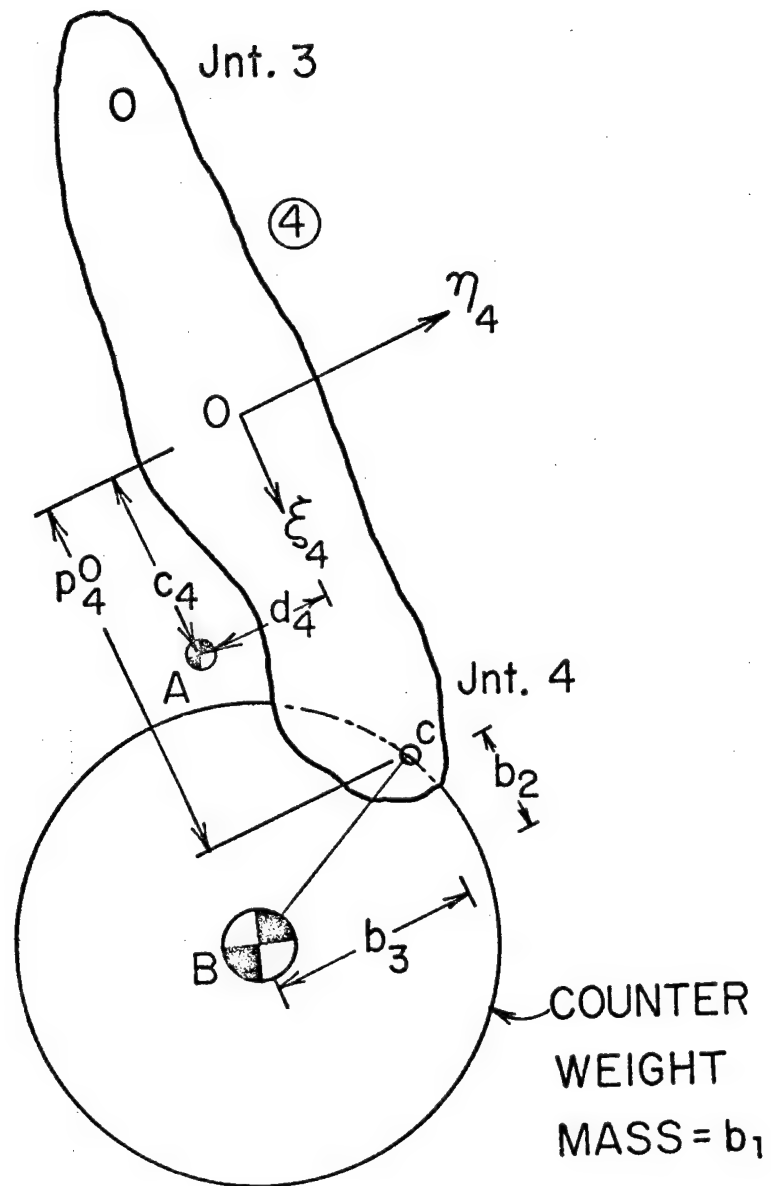Figure 5.7   Four-Bar Mechanism to be Dynamically Balanced

Figue 5.8   Schematic of Counterweight Used in Dynamic Balancing

Table 5.7 Data for Example 5

	LINK			
	1	2	3	4
Length (m)	7.62×10^{-2}	2.54×10^{-2}	1.016×10^{-1}	7.62×10^{-2}
Mass (kg)	--	4.588×10^{-2}	1.084×10^{-1}	6.602×10^{-2}
Moment of inertia @ C.G kg-m^2	--	--	3.208×10^{-4}	6.779×10^{-5}

5.5.2 Problem Formulation

The RMS shaking force for the four-bar mechanism being considered here is given as [4]

$$
\left(F_{M/G}\right)_{RMS} = \sqrt{\frac{1}{2\pi} \int_0^{2\pi} \left[(F_{14X} + F_{34X})^2 + \left[(F_{14Y} + F_{34Y})^2\right]d\theta_2\right.}
$$

(5.32)

where F_{14X} and F_{14Y} are the ground-bearing forces at joint 1, in the X and Y directions, respectively; F_{34X} and F_{34Y} are the ground-bearing forces at joint 4, in the X and Y directions, respectively; and θ_2 is the angular orientation of the input crank.

The RMS ground-bearing forces are given as [4],

$$
\left(F_1\right)_{RMS} = \sqrt{\frac{1}{2\pi} \int_0^{2\pi} \left[(F_{41X}^2 + F_{41Y}^2)\right]d\theta_2}
$$

(5.33)

$$
\left(F_4\right)_{RMS} = \sqrt{\frac{1}{2\pi} \int_0^{2\pi} \left[(F_{43X}^2 + F_{43Y}^2)\right]d\theta_2}
$$

(5.34)

where $\left(F_1\right)_{RMS}$ and $\left(F_4\right)_{RMS}$ are the RMS ground-bearing forces at joints 1 and 4, respectively.

There is a one to one correspondence between the design variables used here and those used in Ref. 4. Location of the center of mass of the combined link, in terms of design variables and given data, can be written, using relationships given in Ref. 4, as

$$
C_4 = p_4^0 - \frac{1}{(m_4^0 + b_1)} \left(m_4^0 p_4^0 - b_1 b_2\right)
$$

(5.35)

and

$$d_4 = \frac{1}{\left(m_4^0 + b_1\right)} \tag{5.36}$$

where c_4 and d_4 define the location of the combined center of mass, b_1 is the mass of the counterweight, b_2 and b_3 are the distances shown in Fig. 5.8, m_4^0 is mass of the original output link, and p_4^0 is given data, as defined in Fig. 5.8.

Acceleration of point A relative to point 0 can be computed by the relation

$$\bar{a}_{A0} = \frac{d^2}{dt^2} \left(\bar{r}_{A0}\right) \tag{5.37}$$

where $\bar{r}_{A0}$ is the position vector of point A, relative to point 0, given as

$$\bar{r}_{A0} = \left(c_4 \cos\theta_4 - d_4\sin\theta_4\right)\bar{I} + \left(c_4\sin\theta_4 + d_4\cos\theta_4\right)\bar{J} \tag{5.38}$$

Substituting $\bar{r}_{A0}$ from Eq. 5.38 into Eq. 5.37 gives

$$\bar{a}_{A0} = \{-\left(c_4 \cos\theta_4 - d_4\sin\theta_4\right)\left(\dot{\theta}_4\right)^2 - \left(c_4 \sin\theta_4 - d_4\cos\theta_4\right)\ddot{\theta}_4 \}\bar{I}$$

$$\{-\left(c_4 \sin\theta_4 + d_4\cos\theta_4\right)\left(\dot{\theta}_4\right)^2 + \left(c_4 \cos\theta_4 - d_4\sin\theta_4\right)\ddot{\theta}_4 \}\bar{J}$$

$$\tag{5.39}$$

The absolute acceleration of point A can thus be written as

$$\bar{a}_A = \bar{a}_0 + \bar{a}_{A0} \tag{5.40}$$

D'Alembert's force on the output link can now be written as

$$\bar{F}_4 = -(m_4^0 + b_1) \, \bar{a}_A \tag{5.41}$$

Computation of D'Alembert moments requires the combined moment of inertia of the original link and the counterweight. Since the counterweight is circular, it's moment of inertia about point B is given as

$$I^* = b_1(b_2^2 + b_3^2)/2 \tag{5.42}$$

Using the parallel axis theorem [23], the combined moment of inertia of the original link and the counterweight can be written as

$$I_A = I_0 + m_4^0(|\bar{r}_{0A}|)^2 + I^* + b_1(|\bar{r}_{AB}|)^2 \tag{5.43}$$

where I_A is the combined moment of inertia about point A and I_0 is the moment of inertia of the original link about point 0. Since moment of inertia of the original link given in Ref. 4 is about point C, the parallel axis theorem must be used to write I_0 in Eq. 5.43 in terms of the given data,

$$I_C = I_0 + m_4^0 (p_4^0)^2 \tag{5.44}$$

Substituting for I_0 in Eq. 5.42 from Eq. 5.44 gives

$$I_A = I_C - m_4^0(p_4^0)^2 + m_4^0(c_4^2 + d_4^2)$$
$$+ I^* + b_1 \left[(p_4^0 - c_4 + b_2)^2 + (b_3 - d_4)^2\right] \tag{5.45}$$

The D'Alemberts moment can now be written as

$$\bar{M} = -I_A \ddot{\theta}_4 \tag{5.46}$$

Forces in the ground bearings, used in Eqs. 5.32 to 5.34, can be related, from the results of Section 3.3.1, to the Lagrange multipliers by the following relationships

$$F_{14X} = -\mu_4$$

$$F_{14Y} = -\mu_5$$

$$F_{34X} = \mu_{10} \tag{5.47}$$

$$F_{34Y} = \mu_{11}$$

Equations 5.32 to 5.34 can thus be rewritten as

$$(F_{M/G})_{RMS} = \sqrt{\frac{1}{2\pi} \int_0^{2\pi} \left[(-\mu_4 + \mu_{10})^2 + (-\mu_5 + \mu_{11})^2 \right] d\theta_2} \tag{5.48}$$

$$(F_1)_{RMS} = \sqrt{\frac{1}{2\pi} \int_0^{2\pi} \left[\mu_4^2 + \mu_5^2 \right] d\theta_2} \tag{5.49}$$

$$(F_4)_{RMS} = \sqrt{\frac{1}{2\pi} \int_0^{2\pi} \left[\mu_{10}^2 + \mu_{11}^2 \right] d\theta_2} \tag{5.50}$$

The optimization problem can now be stated in the standard form of minimizing

$$\psi_0 \equiv (F_{M/G})_{RMS} \tag{5.51}$$

subject to constraints

$$\psi^1 \equiv \frac{(F_1)_{RMS}}{F_1} - 1 \leqslant 0 \tag{5.52}$$

$$\psi^2 \equiv \frac{(F_4)_{RMS}}{F_4} - 1 \leqslant 0 \tag{5.53}$$

where $(F_{M/G})_{RMS}$, $(F_1)_{RMS}$, and $(F_4)_{RMS}$ are given by Eqs. 5.48, 5.49, and 5.50, respectively, and F_1 and F_4 are the upper bounds on the bearing forces at revolute joints 1 and 4, respectively.

The driving kinematic constraint for this problem is

$$\phi_1^d \equiv \theta_2 - \alpha_1^j = 0 \ , \qquad j = 1,\ldots,15$$

The rationale used to compute the values of F_1 and F_4 is explained in detail in Ref. 4. Briefly, to arrive at these numbers the RMS ground bearing forces for the unbalanced mechanism and the fully force balanced mechanism are computed.

Since the RMS bearing forces for the fully force balanced mechanism are higher than those for the unbalanced mechanism, the values of F_1 and F_4 are chosen to lie midway between the two extreme values. For the present, these values are taken as $F_1 = 9.136 \times 10^{-3}$ N and $F_4 = 6.427 \times 10^{-3}$ N.

The cost function and design constraints considered in example problems thus far do not involve integrated quantities such as those appearing in Eqs. 5.48 to 5.50. Computation of design sensitivities of these functions can also be handled by the formulation developed here. Design sensitivities of the integral cost and constraint functions can similarly be written by taking the derivatives with respect to design of Eqs. 5.51 to 5.53 [32], yielding

$$\ell_0^T = \frac{d\psi_0}{db} = \frac{1}{2\pi(F_{M/G})_{RMS}} \int_0^{2\pi} [(-\mu_4 + \mu_{10})(-\frac{d\mu_4}{db} + \frac{d\mu_{10}}{db})$$

$$+ (-\mu_5 + \mu_{11})(-\frac{d\mu_5}{db} + \frac{d\mu_{11}}{db})] \, d\theta_2 \qquad (5.54)$$

$$\ell^{1^T} = \frac{d\psi^1}{db} = F_1 \left\{ \frac{1}{2\pi(F_1)_{RMS}} \int_0^{2\pi} \left[\mu_4 \frac{d\mu_4}{db} + \mu_5 \frac{d\mu_5}{db} \right] d\theta_2 \right\} \qquad (5.55)$$

$$\ell^{2^T} = \frac{d\psi^2}{db} = F_4 \left\{ \frac{1}{2\pi(F_4)_{RMS}} \int_0^{2\pi} \left[\mu_{10} \frac{d\mu_{10}}{db} + \mu_{11} \frac{d\mu_{11}}{db} \right] d\theta_2 \right\} \qquad (5.56)$$

Numerical integration of Eqs. 5.54 to 5.56 requires evaluation of the integrand at specific points in the interval of integration. Computation of the derivatives of Lagrange's multipliers appearing in the integrands of Eqs. 5.54 to 5.56 can be routinely done in the present formulation. The computer code is forced to treat μ_4, μ_5, μ_{10}, and μ_{11} as constraint functions, purely for the purpose of computing the design sensitivity. The design sensitivity of these functions is evaluated at points on the θ_2 grid corresponding to the nodes of the 15 point Gauss–Legendre integration formula [33]. Since constraints ψ^1 and ψ^2 do not depend on the input parameter, they are nonparametric constraints.

5.5.3 Numerical Results

5.5.3.1 Verification of Design Sensitivity Analysis

The design sensitivity vectors of the cost and constraint functions, at a certain design iteration, were obtained as

$$\ell^{0^T} = [-.000799, \ .02880, \ .004828]$$

$$\ell^{1^T} = [4.1542, \ -12.7106, \ 3.1470]$$

$$\ell^{2^T} = [3.9492, \ -14.846, \ -.3122]$$

The change in design in this iteration was

$$\delta b = [-0.000885, \ 0.001334, \ 0.000373]$$

The predicted change in cost is thus computed as

$$\Delta \psi_P^0 = \ell^{0^T} \delta b = 0.0000409$$

Predicted changes in constraints are computed as

$$\Delta \psi_P^1 = -.01946$$

$$\Delta \psi_P^2 = -.0234$$

The actual changes in the cost and constraints were

$$\Delta \psi_A^0 = 0.000057$$

$$\Delta \psi_A^1 = -.011355$$

$$\Delta \psi_A^2 = -.01406$$

Comparing the predicted and actual changes in cost and constraint functions, it can be seen that the two sets of data no not agree well. This can be attributed to the highly nonlinear nature of the cost and constraint functions. This can be seen by computing the predicted change in constraint, using an average design sensitivity vector. For example, consider constraint 1, for which the design sensitivity vector averaged over the two design iterations is

$$[\ell^{1^T}]_{AVE} = [4.1145, \ -12.4848, \ 3.1727]$$

The predicted change in the constraint, on the basis of the averaged design sensitivity vector, is

$$\left[\Delta\psi_p^1\right]_{AVE} = -.01183$$

As can be seen, this figure agrees closely with the actual change in the constraint.

5.5.3.2 Optimization Results

Results obtained from the optimization procedure are presented in Table 5.8. For the purpose of comparison, the design variables used in Ref. 4 are converted to those used in the present formulation. The ratio of the RMS shaking force for the partially balanced mechanism to that for the unbalanced mechanism is given by r_f. As can be seen from Table 5.8, a substantial reduction in RMS shaking force is obtained by using the present formulation. Results obtained from the present formulation and those in Ref. 4 differ substantially. This difference is attributed to the fact that the present formulation imposes the RMS ground bearing force constraints as inequality constraints and Ref. 4 considers these to be equality constraints. Significant improvement in design from the present formulation over that from Ref. 4 is thus to be expected and is evident from Table 5.8.

Table 5.8   Results in Example 5

	Design Variables in present paper			
	b_1 (kg)	b_2 (m)	b_3 (m)	r_f
Starting Design	0.30	0.0	0.0	--
Optimal Design, 15th Iter	0.203	0.040	0.0098	0.25
Optimal Design Ref. 4	0.207	0.0183	-0.017	0.69

At the final design $||\delta b^1|| = 1.6 \times 10^{-4}$

Approximate computing time IBM 370/168 = 1.0 Secs/iteration

CHAPTER 6

CONCLUSIONS AND RECOMMENDATIONS
FOR FURTHER RESEARCH

6.1 Conclusions

The five examples presented in Chapter 5 were studied to evaluate versatility and effectiveness of the technique developed in the previous chapters. In light of the results obtained with these examples, the following conclusions may be drawn:

1. The constrained multi-element technique developed in Chapters 2 and 3 for modeling kinematic systems is general enough to represent a wide variety of planar mechanisms.

2. The adjoint variable technique has been successfully applied for design sensitivity analaysis of planar mechanisms, considering both kinematic and force response of mechanisms.

3. Due to the generality of the constrained multi-element technique for modeling and the adjoint variable technique for design sensitivity analysis, the synthesis and design technique developed in this research is very general and versatile. This is evident from the variety of examples given in Chapter 5.

6.2 Recommendations for Further Research

In the preceding section it was pointed out that the state space technique developed in this research has demonstrated its potential

as a versatile and powerful tool for kinematic synthesis and design. However, to fully realize this potential, it is recommended that the following areas be further investigated:

1. The gradient projection algorithm stated in Chapter 5 was used as the optimization algorithm in this research. This algorithm, in its present form, is insensitive to nonlinearity of the state equations and in the cost and constraint functions encountered in kinematic synthesis and design problems. In addition to its insensitivity to nonlinearities, this optimization algorithm often produces designs for which the mechanism locks up in some position. This is primarily due to the algorithm's not having any information about the kinematics of the mechanism.

    It is thus desirable to investigate alternate optimization algorithms that have the following desirable characteristics:

    (i) The algorithm should be sensitive to nonlinearities arising in mechanism synthesis and design problems.

    (ii) The algorithm should produce design changes that are compatible with kinematic requirements of the mechanism.

2. The gradient projection algorithm, like many other optimization algorithms, does not guarantee a globally optimal design. To be assured that the optimal design produced by the optimization technique is globally optimal, it is necessary to start the procedure with different initial designs. In most mechanism synthesis problems a substantial effort has to be

put into producing acceptable initial designs. It is thus desirable to investigate techniques that guarantee convergence to globally optimal designs.

3.   The computer code used to implement the theory developed in the previous chapters was of an experimental nature. Some of the areas in which this code could be refined are as follows:

(i)   Significant improvements should be made in the solution procedure for state equations.

(ii) Computation of derivatives of user-supplied driving kinematic equations and cost and constraint functions should be carried out with a symbolic manipulation language.

(iii) Implementation of the code for execution in a conversational mode would be highly desirable.

4.   Synthesis and design of three-dimensional mechanisms is currently at an elementary level. The theory developed here for synthesis and design of planar mechanisms is extendable to three-dimensional mechanisms and should be pursued.

REFERENCES

1. Freudenstein, F., "Structural Error Analysis in Plane Kinematic Synthesis," ASME, Journal of Engineering for Industry, Ser. B, Vol. 81, No. 1, Feb. 1959, pp. 15-22.

2. Kramer, S.N. and Sandor, G.N., "Selective Precision Synthesis - A General Method of Optimization for Planar Mechanisms," ASME, Journal of Engineering for Industry, Ser. B, Vol. 97, No. 2, 1975.

3. Tepper, F.R. and Lowen, G.G., "General Theorems Concerning Full Force Balancing of Planar Linkages by Internal Mass Redistribution, ASME, Journal of Engineering for Industry, Ser. B, Vol. 94, No. 3, Aug. 1972, pp. 789-796.

4. Tepper, F.R. and Lowen, G.G., "Shaking Force Optimization of Four-Bar Linkage with Adjustable Constraints on Ground Bearing Forces," ASME, Journal of Engineering for Industry, Ser. B, Vol. 97, No. 2, May 1975, pp. 643-651.

5. Berkof, R.S., "Force Balancing of a Six-Bar Linkage," Proceedings of the Fifth World Congress on the Theory of Machines and Mechanisms, July 8-13, 1979, Montreal, Canada, pp. 1082-1085.

6. Ramaiyan, G. and Lakshminarayan, K., "Synthesis of Seven Link Two-Freedom Linkage with Sliding Inputs and Outputs using Identical Link Positions," Mechanisms and Machine Theory, Vol. 11, No. 3, 1976, pp. 181-185.

7. Ramaiyan, G., Lakshminarayan, K. and Narayanamurthi, R.G., "Nine-Link Plane Mechanisms for Two-Variable Function Generation - II. Synthesis," Mechanisms and Machine Theory, Vol. 11, No. 3, 1976, pp. 193-199.

8. Mariante, W. and Willmert, K.D., "Optimal Design of a Complex Planar Mechanism," ASME, Journal of Engineering for Industry, Ser. B, Vo. 99, No. 3, Aug. 1977, pp. 539-546.

9. Thronton, W.A., Willmert, K.D., and Khan, M.R., "Mechanism Optimization via Optimality Criterion Techniques," Journal of Mechanical Design, Trans. ASME, Vol. 101, No. 1, July 1979, pp. 392-397.

10. Rubel, A.J. and Kaufman, R.E., 'KINSYN III: A New Human Engineered System for Interactive Computer Aided Design of Planar Linkages," ASME, Journal of Engineering for Industry, Vol. 99, No. 2, March 1977, pp. 440-455.

11. Rucci, R. J. "SPACEBAR: Kinematic Design by Computer Graphics," Computer Aided Design, Vol. 8, No. 4, October 1976, pp. 219-226.

12. Erdman, A.G. and Gustavson, J.E. "LINCAGES: Linkage Interactive Computer Analysis and Graphically Enhanced Synthesis Package," ASME paper 77-DET-5.

13. Paul, B., "Analytical Dynamics of Mechanisms - A Computer Related Overview," Mechanism and Machine Theory, Vol. 10, No. 4, 1975, pp. 481-507.

14. Hartenberg, R.S. and Denavit, J., Kinematic Synthesis of Linkages," McGraw-Hill Book Co., 1964.

15. Sheth, P.N. and Uicker, J.J., 'IMP Integrated Mechanism Program], A Computer Aided Design System for Mechanisms and Linkages," Journal of Engineering for Industry, Trans. ASME, Vol. 93, No. 4, 1971.

16. Paul, B., Kinematics and Dynamics of Planar Machinery, Prentice-Hall, 1979.

17. Orlandea N., Chace, M.A. and Calahan, D.A., "A Sparsity-Oriented Approach to the Dynamic Analysis and Design of Mechanical Systems," Part I and II, ASME, Journal of Engineering for Industry, Ser. B., Vol. 99, No. 3, 1977.

18. Wehage, R.A. and Haug, E.J., "Generalized Coordinate Partitioning for Dimension Reduction in Analysis of Constrained Dynamic Systems," ASME paper no. 80-DET-106. To be published in Journal of Mechanical Design.

19. Haug, E.J., Wehage, R. and Barman, N.C., "Design Sensitivity Analysis of Planar Mechanism and Machine Dynamics," ASME, Journal of Mechanical Design, Vol. 103, No. 3, pp. 560-570, 1981.

20. Haug, E.J. and Arora, J.S., Applied Optimal Design, John Wiley & Sons, 1979.

21. Atkinson, K.E., An Introduction to Numerical Analysis, John Wiley & Sons, 1978.

22. United Kindgom Atomic Energy Authority: "Harwell Subroutine Library: A Catalogue of Subroutines," Report AERE R7477, Subroutine Librarian, CSS Division, Atomic Energy Research Establishment, Harwell Didcot, Oxfordshire, England OX11 ORA, 1973.

23. Greenwood, D.T., Principles of Dynamics, Prentice-Hall, 1965.

24. Goldstein, H., Classical Mechanics, 2nd ed., Addison-Wesley Publishing Company, 1980.

25. Kwak, B.M., Parametric Optimal Design, Ph.D. Thesis, University of Iowa, Iowa, City, 1975.

26. Kwak, B.M. and Haug, E.J. "Optimal Synthesis of Planar Mechanisms by Parametric Design Techniques," Engineering Optimization, 1976, Vol. 2, pp. 55-63.

27. Sohoni, V. and Haug, E.J., "A State Space Method for Kinematic Synthesis of Mechanisms and Machines, ASME paper No. 80-DET-43. To be published J. of Mechanical Design, ASME, 1981.

28. Bhatia, D.H. and Bacci, C., "Optimal Synthesis of Multiloop Planar Mechanisms for the Generation of Paths and Rigid Body Positions by the Linear Partition of Design Equations," ASME paper No. 74-DET-14.

29. Khan, M.R., Thornton, W.A. and Willmert, K.D., "Optimality Criterion Techniques Applied to Mechanical Design," Journal of Mechanical Design, ASME, Vol. 100, April 1978, pp. 319-321.

30. Imam, I. and Sandor, G.N., "A General Method of Kineto-Elastodynamic Design of High Speed Mechanisms," Mechanicisms and Machine Theory, Vol. 8, 1973, pp. 497-516.

31. Ugural, A.C. and Fenster, S.K., Advanced Strength and Applied Elasticity, American Elsevier Publishing Company, 1975.

32. Taylor, A.E. and Mann, W.R., Advanced Calculus, Wiley, 1972.

33. Carnahan, B., Luther, H.A. and James, W.O., Applied Numerical Methods, John Wiley & Sons, 1969.

APPENDIX A

PROOF OF NONSINGULARITY OF MATRIX A IN EQUATION 4.27

Matrix A^j defined in Eq. 4.27 is the coefficient matrix on the left-hand side of Eq. 4.26. A proof of the existance of an inverse for this matrix will now be developed. The Jacobian matrix $(\partial \Phi / \partial z)_j$ that occupies a band along the diagonal of matrix A is assumed to be nonsingular. This assumption is initially made in Section 2.2.3 and is still valid here.

Consider Eq. 4.22, with perturbation in design $\delta b = 0$,

$$\left[\frac{\partial \Phi}{\partial z}\right]_j \delta z^j = 0 \tag{A.1}$$

Since the coefficient matrix of Eq. A.1 is nonsingular, by theorem 7.2 of Ref. 21, Eq. A.1 implies that

$$\delta z^j = 0 \tag{A.2}$$

Consider Eq. 4.23 with $\delta b = 0$,

$$\left[\frac{\partial \Phi}{\partial z}\right]_j \delta \dot{z}^j = -\left\{\frac{\partial}{\partial z}\left[\frac{\partial \Phi}{\partial z}\dot{z}\right] + \frac{\partial}{\partial z}\left[\frac{\partial \Phi}{\partial \alpha}\dot{\alpha}\right]\right\}_j \delta z^j \tag{A.3}$$

Substituting for δz^j from Eq. A.2, Eq. A.3 becomes

$$\left[\frac{\partial \Phi}{\partial z}\right]_j \delta \dot{z}^j = 0 \tag{A.4}$$

By the same argument, Eq. A.4 implies

$$\delta \dot{z}^j = 0 \tag{A.5}$$

Consider Eq. 4.24 with $\delta b = 0$ and Eqs. A.2 and A.5,

$$\left[\frac{\partial \Phi}{\partial z}\right]_j \delta \ddot{z}^j = 0 \tag{A.6}$$

As deduced previously, Eq. A.6 implies

$$\delta \ddot{z}^j = 0 \tag{A.7}$$

Consider Eq. 4.25 with $\delta b = 0$ and Eqs. A.2, A.5 and A.7,

$$\left[\frac{\partial \Phi}{\partial z}\right]_j^T \delta \mu^j = 0 \tag{A.8}$$

The coefficient matrix of Eq. A.8 is the transpose of the Jacobian matrix of Eq. A.1. Since the Jacobian is nonsingular, its transpose also has the same property. Eq. A.8 thus implies

$$\delta \mu^j = 0 \tag{A.9}$$

From the definition of the composite state variable vector U^j given in Section 4.3,

$$\delta U^{j^T} = \left[\delta z^T \ \middle| \ \delta \dot{z}^T \ \middle| \ \delta \ddot{z}^T \ \middle| \ \delta \mu^T\right]_j^T \tag{A.10}$$

Substituting from Eqs. A.2, A.5, A.7 and A.9, Eq. A.10 can be written as

$$\delta U^j = \bar{0} \tag{A.11}$$

Now consider Eq. 4.27 with $\delta b = 0$,

$$A^j \delta U^j = \bar{0} \tag{A.12}$$

As shown in the above, Eq. A.12 implies that Eq. A.11 holds, i.e.,

$$\delta \ U^{j} \ = \ 0$$

By theorem, 7.2 of Ref. 21, this is equivalent to the statement that (A^{j}) is nonsingular.

APPENDIX B

DERIVATIVES OF KINEMATIC CONSTRAINT EQUATIONS

B.1 Notation

Before any derivatives of Kinematic Constraint Equations are
calculated, the following notation is introduced for a revolute joint§

$$
\left.
\begin{aligned}
R_1 &= \xi_{ij} \cos \theta_i - \eta_{ij} \sin \theta_i \\[2ex]
R_2 &= \xi_{ij} \sin \theta_i + \eta_{ij} \cos \theta_i \\[2ex]
R_3 &= \xi_{ji} \cos \theta_j - \eta_{ji} \sin \theta_j \\[2ex]
R_4 &= \xi_{ji} \sin \theta_j - \eta_{ji} \cos \theta_j
\end{aligned}
\right\}
\qquad (B.1)
$$

$$
\left.
\begin{aligned}
RB1 &= \frac{\partial R_1}{\partial b_k} = \frac{\partial \xi_{ij}}{\partial b_k} \cos \theta_i - \frac{\partial \eta_{ij}}{\partial b_k} \sin \theta_i \\[2ex]
RB2 &= \frac{\partial R_2}{\partial b_k} = \frac{\partial \xi_{ij}}{\partial b_k} \sin \theta_i - \frac{\partial \eta_{ij}}{\partial b_k} \cos \theta_i \\[2ex]
RB3 &= \frac{\partial R_3}{\partial b_k} = \frac{\partial \xi_{ji}}{\partial b_k} \cos \theta_j - \frac{\partial \eta_{ji}}{\partial b_k} \sin \theta_j \\[2ex]
RB4 &= \frac{\partial R_4}{\partial b_k} = \frac{\partial \xi_{ji}}{\partial b_k} \sin \theta_j + \frac{\partial \eta_{ji}}{\partial b_k} \cos \theta_j
\end{aligned}
\right\}
\qquad (B.2)
$$

The partial derivatives $\dfrac{\partial \xi_{ij}}{\partial b_k}$, $\dfrac{\partial \eta_{ij}}{\partial b_k}$, $\dfrac{\partial \xi_{ji}}{\partial b_k}$ and $\dfrac{\partial \eta_{ji}}{\partial b_k}$, will take on

nonzero values only if design variable b_k is related to the lengths of body i or j.

Similarly for translational joint, the following notation is introduced:

$$
\begin{aligned}
T1 &= \xi_{ij} \cos \theta_i - \eta_{ij} \sin \theta_i \\[2mm]
T2 &= \xi_{ij} \sin \theta_i + \eta_{ij} \cos \theta_i \\[2mm]
T3 &= \xi_{ji} \cos \theta_j - \eta_{ji} \sin \theta_j \\[2mm]
T4 &= \xi_{ji} \sin \theta_j + \eta_{ji} \cos \theta_j \\[2mm]
T5 &= (T1)(T3) + (T2)(T4) \\[2mm]
T6 &= -(T2)(T3) + (T1)(T4) \\[2mm]
T7 &= x_i - x_j \\[2mm]
T8 &= y_i - y_j
\end{aligned}
\qquad (B.3)
$$

$$
\begin{aligned}
TB1 &= \frac{\partial T1}{\partial b_k} = \frac{\partial \xi_{ij}}{\partial b_k} \cos \theta_i - \frac{\partial \eta_{ij}}{\partial b_k} \sin \theta_i \\[4mm]
TB2 &= \frac{\partial T2}{\partial b_k} = \frac{\partial \xi_{ij}}{\partial b_k} \sin \theta_i + \frac{\partial \eta_{ij}}{\partial b_k} \cos \theta_i \\[4mm]
TB3 &= \frac{\partial T3}{\partial b_k} = \frac{\partial \xi_{ji}}{\partial b_k} \cos \theta_j - \frac{\partial \eta_{ji}}{\partial b_k} \sin \theta_j
\end{aligned}
\qquad (B.4)
$$

$$TB4 = \frac{\partial T4}{\partial b_k} = \frac{\partial \xi_{ji}}{\partial b_k} \sin \theta_j + \frac{\partial \eta_{ji}}{\partial b_k} \cos \theta_j$$

$$TB5 = (TB1)(T3) + (T1)(TB3) + (TB2)(T4) + (T2)(TB4)$$

$$TB6 = - (TB2)(T3) - (T2)(TB3) + (TB1)(T4) + (T1)(TB4)$$

The partial derivatives $\dfrac{\partial \xi_{ij}}{\partial b_k}$, $\dfrac{\partial \eta_{ij}}{\partial b_k}$, $\dfrac{\partial \xi_{ji}}{\partial b_k}$ and $\dfrac{\partial \eta_{ji}}{\partial b_k}$ in Eq. B.4 will take on non-zero values only if the design variable b_k is related to location of the translational joint connecting bodies i and j.

B.2   Derivatives With Respect To Design Variables Only

Consider now each of the two types of joints separately.

B.2.1   Revolute Joint

From Eqs. 2.10 the derivative of constraint equations with respect to design variables could be written as

$$\frac{\partial \phi_x}{\partial b_k} = RB1 - RB3$$

$$\frac{\partial \phi_y}{\partial b_k} = RB2 - RB4$$

$$(B.5)$$

where RB1, RB2, RB3 and RB4 are defined by Eq. B.2

B.2.2   Translational Joint

From Eqs. 2.13 and 2.16, the derivatives of the constraint equations for the translational joint with respect to design can be written as

$$\frac{\partial \phi_n}{\partial b_k} = (TB1)(U_i - U_j) + (U_i - x_i)(TB1 - TB3) +$$

$$(TB2)(V_i - V_j) + (V_i - y_i)(TB2 - TB4)$$

$$\frac{\partial \phi_\theta}{\partial b_k} = (TB1)(V_j - y_j) + (U_i - x_i)(TB4) -$$

$$(TB2)(U_j - x_j) + (V_i - y_i)(TB3)$$

$$(B.6)$$

where TB1, TB2, TB3 and TB4 are given by Eqs. B.4 and U_i, U_j, V_i and V_j are given by Eqs. 2.14.

B.3   Derivatives With Respect To State Variables

B.3.1 First-Order Partial Derivatives

B.3.1.1   Revolute Joint

From Eq. 2.10, the nonzero first-order partial derivatives of equations of constraint for the revolute joint can be written as

$$\frac{\partial \phi_x}{\partial x_i} = 1$$

$$\frac{\partial \phi_x}{\partial \theta_i} = -R2$$

$$\frac{\partial \phi_x}{\partial x_j} = -1$$

$$\frac{\partial \phi_x}{\partial \theta_j} = R4$$

$$(B.7)$$

$$\frac{\partial \phi_y}{\partial y_i} = 1$$

$$\frac{\partial \phi_y}{\partial \theta_i} = R1$$

$$\frac{\partial \phi_y}{\partial y_j} = -1$$

$$\frac{\partial \phi_y}{\partial \theta_j} = -R3$$

B.3.1.2   Translational Joint

From Eqs. 2.13 and 2.16, the nonzero first-order partial derivatives of the equations of constraint for a translational joint can be written as

$$\frac{\partial \phi_n}{\partial x_i} = T1$$

$$\frac{\partial \phi_n}{\partial y_i} = T2$$

$$\frac{\partial \phi_n}{\partial \theta_i} = -(T2)(T7) + (T1)(T8) - T6$$

$$\frac{\partial \phi_n}{\partial x_j} = -T1$$

$$\frac{\partial \phi_n}{\partial y_j} = -T2$$

(B.8)

$$\frac{\partial \phi_n}{\partial \theta_j} = T6$$

$$\frac{\partial \phi_\theta}{\partial \theta_i} = - T5$$

$$\frac{\partial \phi_\theta}{\partial \theta_j} = T5$$

B.3.2   Second-Order Partial Derivatives

B.3.2.1   Revolute Joint

Differentiating the derivatives in Eq. B.7 once with respect to the state variables gives the following nonzero second derivatives:

$$\frac{\partial^2 \phi_x}{\partial \theta_i^2} = - R1$$

$$\frac{\partial^2 \phi_x}{\partial \theta_j^2} = R3$$

$$\frac{\partial^2 \phi_y}{\partial \theta_i^2} = - R2$$

$$\frac{\partial^2 \phi_y}{\partial \theta_j^2} = R4$$

(B.9)

B.3.2.2 Translational Joint

Differentiating the derivatives in Eq. B.8 with respect to state variables gives the following nonzero second derivatives:

$$\frac{\partial^2 \phi_n}{\partial x_i \, \partial \theta_i} = -T2$$

$$\frac{\partial^2 \phi_n}{\partial y_i \, \partial \theta_i} = T2$$

$$\frac{\partial^2 \phi_n}{\partial \theta_i \, \partial x_j} = T2$$

$$\frac{\partial^2 \phi_n}{\partial \theta_i \, \partial y_j} = -T2$$

$$\frac{\partial^2 \phi_n}{\partial \theta_i \, \partial \theta_j} = T5$$

$$\frac{\partial^2 \phi_n}{\partial \theta_i^2} = -(T1)(T7) - (T2)(T8) + T5$$

$$\frac{\partial^2 \phi_n}{\partial \theta_j^2} = T5$$

(B.10)

$$\frac{\partial^2 \phi_\theta}{\partial \theta_i^{\,2}} = - \text{T6}$$

$$\frac{\partial^2 \phi_\theta}{\partial \theta_i \partial \theta_j} = \text{T6}$$

$$\frac{\partial^2 \phi_\theta}{\partial \theta_j^{\,2}} = - \text{T6}$$

B.3.3 Third-Order Partial Derivatives

B.3.3.1 Revolute Joint

Differentiating Eq. B.9 once with respect to state variables gives the following nonzero third derivatives:

$$\frac{\partial^3 \phi_x}{\partial \theta_i^{\,3}} = \text{R2}$$

$$\frac{\partial^3 \phi_x}{\partial \theta_j^{\,3}} = - \text{R4}$$

$$\frac{\partial^3 \phi_y}{\partial \theta_i^{\,3}} = - \text{R1}$$

(B.11)

$$\frac{\partial^3 \phi_y}{\partial \theta_j^3} = R3$$

B.3.3.2 Translational Joint

Differentiating Eq. B.10 once with respect to state variables gives the following nonzero third derivatives:

$$\frac{\partial^3 \phi_n}{\partial x_i \, \partial \theta_i^2} = - T1$$

$$\frac{\partial^3 \phi_n}{\partial y_i \, \partial \theta_i^2} = - T2$$

$$\frac{\partial^3 \phi_n}{\partial x_j \, \partial \theta_i^2} = T1$$

$$\frac{\partial^3 \phi_n}{\partial y_j \, \partial \theta_i^2} = T2$$

$$\frac{\partial^3 \phi_n}{\partial \theta_j \, \partial \theta_i^2} = - T6$$

$$\frac{\partial^3 \phi_n}{\partial\theta_i \partial\theta_j^2} = T6$$

$$\frac{\partial^3 \phi_n}{\partial\theta_i^3} = (T2)(T7) - (T1)(T8) + T6$$

$$\frac{\partial^3 \phi_n}{\partial\theta_j^3} = T6$$

$$\frac{\partial^3 \phi_\theta}{\partial\theta_i^3} = T5$$

$$\frac{\partial^3 \phi_\theta}{\partial\theta_i^2 \partial\theta_j} = -T5$$

$$\frac{\partial^3 \phi_\theta}{\partial\theta_i \partial\theta_j^2} = T5$$

$$\frac{\partial^3 \phi_\theta}{\partial\theta_j^3} = -T5$$

(B.12)

B.4 Cross Derivatives With Respect
to Design and State Variables

B.4.1 Second-Order Cross Partial Derivatives

B.4.1.1 Revolute Joint

Differentiating Eqs. B.7 once with respect to design variables the following nonzero second-order cross partial derivatives result:

$$
\frac{\partial^2 \phi_x}{\partial \theta_i \, \partial b_k} = - RB2
$$

$$
\frac{\partial^2 \phi_x}{\partial \theta_j \, \partial b_k} = - RB1
$$

$$
\frac{\partial^2 \phi_y}{\partial \theta_i \, \partial b_k} = - RB4
$$

$$
\frac{\partial^2 \phi_y}{\partial \theta_j \, \partial b_k} = - RB3
$$

$$
\frac{\partial^2 \phi_\theta}{\partial \theta_i \, \partial b_k} = - TB5
$$

$$
\frac{\partial^2 \phi_\theta}{\partial \theta_j \, \partial b_k} = TB5
$$

$$(B.13)$$

B.4.1.2 Translational Joint

Differentiating Eq. B.8 with respect to design the following nonzero second-order cross partial derivatives result:

$$\frac{\partial^2 \phi_n}{\partial x_i \, \partial b_k} = TB1$$

$$\frac{\partial^2 \phi_n}{\partial y_i \, \partial b_k} = TB2$$

$$\frac{\partial^2 \phi_n}{\partial \theta_i \, \partial b_k} = -\,(TB2)(T7) - (T2)(TB7) + (TB1)(T8) + (T1)(TB8) - TB6$$

$$\frac{\partial^2 \phi_n}{\partial x_j \, \partial b_k} = -\,TB1$$

$$\frac{\partial^2 \phi_n}{\partial y_j \, \partial b_k} = -\,TB2$$

$$\frac{\partial^2 \phi_n}{\partial \theta_j \, \partial b_k} = TB6$$

(B.14)

B.4.2 Third-Order Cross Partial Derivatives

B.4.2.1 Revolute Joint

Differentiating the second-order derivatives in Eq. B.9 once with respect to design gives the following nonzero third-order cross partial derivatives:

$$
\left.
\begin{aligned}
\frac{\partial^3 \phi_x}{\partial\theta_i^2 \, \partial b_k} &= -\, RB1 \\[2em]
\frac{\partial^3 \phi_x}{\partial\theta_j^2 \, \partial b_k} &= \quad RB3 \\[2em]
\frac{\partial^3 \phi_y}{\partial\theta_i^2 \, \partial b_k} &= -\, RB2 \\[2em]
\frac{\partial^3 \phi_y}{\partial\theta_j^2 \, \partial b_k} &= \quad RB4
\end{aligned}
\right\}
\qquad (B.15)
$$

B.4.2.2 Translational Joint

Differentiating the second-order derivatives in Eq. B.10 once with respect to design gives the following nonzero third-order partial cross derivatives:

$$
\left.
\frac{\partial^3 \phi_n}{\partial x_i \, \partial\theta_i \, \partial b_k} = -\, TB2
\right]
$$

$$\frac{\partial^3 \phi_n}{\partial y_i \, \partial \theta_i \, \partial b_k} = TB2$$

$$\frac{\partial^3 \phi_n}{\partial \theta_i \, \partial x_j \, \partial b_k} = - TB2$$

$$\frac{\partial^3 \phi_n}{\partial x_i \, \partial y_j \, \partial b_k} = - TB2$$

$$\frac{\partial^3 \phi_n}{\partial \theta_i \, \partial \theta_j \, \partial b_k} = TB5$$

$$\frac{\partial^3 \phi_n}{\partial \theta_i^2 \, \partial b_k} = - (TB1)(T7) - (T1)(TB7) - (TB2)(T8)$$
$$+ (T2)(TB8) + TB5$$

$$\frac{\partial^3 \phi_n}{\partial \theta_j^2 \, \partial b_k} = TB5$$

$$\frac{\partial^3 \phi_n}{\partial \theta_i^2 \, \partial b_k} = - TB6$$

$$\frac{\partial^3 \phi_n}{\partial \theta_i \, \partial \theta_j \, \partial b_k} = TB6$$

(B.16)

$$\frac{\partial^3 \phi_n}{\partial \theta_j^2 \, \partial b_k} = - \text{TB6}$$

DISTRIBUTION LIST

Please notify USATACOM, DRSTA-ZSA, Warren, Michigan 48090, of corrections and/or changes in address.

Commander (25)
US Army Tk-Autmv Command
R&D Center
Warren, MI 48090

Superintendent (02)
US Military Academy
ATTN: Dept of Engineering
      Course Director for
      Automotive Engineering

Commander (01)
US Army Logistic Center
Fort Lee, VA 23801

US Army Research Office (02)
P.O. Box 12211
ATTN: Dr. F. Schmiedeshoff
      Dr. R. Singleton
Research Triangle Park, NC 27709

HQ, DA (01)
ATTN: DAMA-AR
      Dr. Herschner
Washington, D.C. 20310

HQ, DA (01)
Office of Dep Chief of Staff
for Rsch, Dev & Acquisition
ATTN: DAMA-AR
      Dr. Charles Church
Washington, D.C. 20310

HQ, DARCOM
5001 Eisenhower Ave.
ATTN: DRCDE
      Dr. R.L. Haley
Alexandria, VA 22333

Director (01)
Defense Advanced Research
Projects Agency
1400 Wilson Boulevard
Arlington, VA 22209

Commander (01)
US Army Combined Arms Combat
Developments Activity
ATTN: ATCA-CCC-S
Fort Leavenworth, KA 66027

Commander (01)
US Army Mobility Equipment
Research and Development Command
ATTN: DRDME-RT
Fort Belvoir, VA 22060

Director (02)
US Army Corps of Engineers
Waterways Experiment Station
P.O. Box 631
Vicksburg, MS 39180

Commander (01)
US Army Materials and Mechanics
Research Center
ATTN: Mr. Adachi
Watertown, MA 02172

Director (03)
US Army Corps of Engineers
Waterways Experiment Station
P.O. Box 631
ATTN: Mr. Nuttall
Vicksburg, MS 39180

Director (04)
US Army Cold Regions Research
& Engineering Lab
P.O. Box 282
ATTN: Dr. Freitag, Dr. W. Harrison
Dr. Liston, Library
Hanover, NH 03755

President   (02)
Army Armor and Engineer Board
Fort Knox, KY   40121

Commander   (01)
US Army Arctic Test Center
APO 409
Seattle, WA   98733

Commander   (02)
US Army Test & Evaluation
Command
ATTN: AMSTE-BB and AMSTE-TA
Aberdeen Proving Ground, MD
21005

Commander   (01)
US Army Armament Research
and Development Command
ATTN: Mr. Rubin
Dover, NJ   07801

Commander   (01)
US Army Yuma Proving Ground
ATTN: STEYP-RPT
Yuma, AZ   85364

Commander   (01)
US Army Natic Laboratories
ATTN: Technical Library
Natick, MA   01760

Director   (01)
US Army Human Engineering Lab
ATTN: Mr. Eckels
Aberdeen Proving Ground, MD
21005

Director   (02)
US Army Ballistic Research Lab
Aberdeen Proving Ground, MD
21005

Director   (02)
US Army Materiel Systems
Analysis Agency
ATTN: AMXSY-CM
Aberdeen Proving Ground, MD
21005

Director   (02)
Defense Documentation Center
Cameron Station
Alexandria, VA   22314

US Marine Corps   (01)
Mobility & Logistics Division
Development and Ed Command
ATTN: Mr. Hickson
Quantico, VA   22134

Keweenaw Field Station (01)
Keweenaw Research Center
Rural Route 1
P.O. Box 94-D
ATTN: Dr. Sung M. Lee
Calumet, MI   49913

Naval Ship Research &   (02)
Dev Center
Aviation & Surface Effects Dept
Code 161
Washington, D.C.   20034

Director   (01)
National Tillage Machinery Lab
Box 792
Auburn, AL   36830

Director   (02)
USDA Forest Service Equipment
Development Center
444 East Bonita Avenue
San Dimes, CA   91773

Engineering Societies   (01)
Library
345 East 47th Street
New York, NY   10017

Dr. I.R. Erlich   (01)
Dean for Research
Stevens Institute of Technology
Castle Point Station
Hoboken, NJ   07030